e-Prime - Advances in Electrical Engineering, Electronics and Energy 10 (2024) 100808

Contents lists available at ScienceDirect

e-Prime - Advances in Electrical Engineering, Electronics and Energy

journal homepage: www.elsevier.com/locate/prime

Off-grid PV/biomass/DG/battery hybrid renewable energy as a source of electricity for a farm facility

Michael Uzoamaka Emezirinwune [a,c,*], Isaiah Adediji Adejumobi [a,c], Oluwaseun Ibrahim Adebisi [a,c], Festus Gboyega Akinboro [b,c]

[a] Department of Electrical/Electronic Engineering, College of Engineering, Nigeria
[b] Department of Physics, College of Physical Sciences, Nigeria
[c] Federal University of Agriculture, Abeokuta, Nigeria

ARTICLE INFO

Keywords:
Photovoltaic
Wind turbine
Biomass
Battery
Hybrid renewable energy system

ABSTRACT

Reliable, cost-effective energy systems are pivotal for sustainable development in the agricultural sector. Using the energy balance analysis of the Hybrid Optimization Model for Electric Renewable (HOMER), this study presents a techno-economic assessment of a hybrid renewable energy system for a farm facility. The energy system components considered in the analysis include solar photovoltaics, wind turbines, diesel generators, biomass, and battery storage. The results shows that ten feasible energy systems can technically power the typical farm facility, with a PV-Biomass-DG battery being the best in terms of the total net present cost. The PV-Biomass-DG-battery systems consist of 561.023 kW of PV, 88 kW of diesel generator, 10 kW of biomass, 81 kW of converter, and 584 batteries operated in a load-following mode. When the cost of energy (COE) of EA1 0.206325 \$/kWh is compared to EA7 0.407681 \$/kWh, a difference of \$0.201356 will be saved for every kWh. Also, a comparison of the operating cost of EA1, \$65,713.23 and the operating cost of EA7 \$212,027.4 showed a margin of \$146,314.17 being saved. Energy systems EA3 and EA4 had the lowest carbon dioxide production levels of 15.8 kg annually, respectively. The simple payback period metrics increased from EA1 to EA6 between 2.97 years to 6.99 years. The result of the study shows that adopting a low-carbon energy transition is technically and economically viable for the agricultural sector, especially in developing countries.

Introduction

Socio-economic activities are driven by reliable access to energy, particularly electricity. The global energy demand is increasing due to population growth and industrialization [1,2]. The increase in energy demand results from the impact of access to energy on enabling economic growth. According to the EIA report [3], by 2050, global energy consumption will rise by over 50%, with Asia leading the way. Also, for the world to achieve significant climate targets by 2050, increased usage of renewable energy along with enhanced electrification may be crucial [4]. There is a link between electricity access and diverse social and economic variables [5]. Over 580 million people in Africa do not have access to electricity [6]. Nigeria is not isolated from this problem of epileptic access to electricity. The problem is more predominant in rural areas and communities with little or no electricity access. According to the latest World Bank report, 73.7% of people in rural Nigeria have no access to electricity [7]. This is in addition to the country's unreliable and dilapidated electricity infrastructure [8]. Due to the epileptic power supply, there is an increase in the number of diesel and petrol electrical power generators in the country [9,10]. Using fossil fuel generators has adverse effects on the environment; it is non-renewable and typically leads to rising operational costs [11]. Also, the emissions from these generators significantly contribute to the rising impacts of climate change [12,13].

The growing evidence of climate change is affecting economies globally [14], there is a need to combat the menace, especially during electricity generation, to reduce the amount of carbon and other pollutants generated [15,16]. To achieve this objective, embracing renewable energy generation is necessary to solve the growing energy demand [17,18]. This method of energy generation will assist globally in eradicating the fossil fuel method of energy generation if adopted [19]. Several pieces of literature have elaborated on the need for an increase in the renewable energy method of electricity generation, its efficiency, and cost-effectiveness compared to the usual method of energy generation [20,21]. By the end of 2023, the global installed capacity for

* Corresponding author.
E-mail address: michaelemezirinwune@yahoo.com (M.U. Emezirinwune).

https://doi.org/10.1016/j.prime.2024.100808
Received 20 June 2024; Received in revised form 27 August 2024; Accepted 7 October 2024
Available online 11 October 2024

List of Nomenclature

Abbreviation/Symbol

PV	Photovoltaic
DG	Diesel Generator
HOMER	Hybrid Optimization Model for Electric Renewable
NPC	Net Present Cost
COE	Cost of Energy
EA	Energy Alternative
LOEP	Loss of Energy Probability
CRF	Capital Recovery Factor
NASRDA	National Space Research and Development Agency
LCA	Life Cycle Assessment
SOC	State of Charge
O&M	Operation and Maintenance
kW	Kilowatt
kWh	Kilowatt-hour
CO2	Carbon Dioxide
η	Efficiency
ρ	Density
β	Power Law Exponent
σ	Self-discharge Rate

renewable energy sources—including solar, wind, hydropower, geothermal, marine, biogas, and others—reached around 3372 GW [22]. The global renewable energy market is projected to continue its upward trajectory in the coming years, growing at a rate of 4.22%. This expansion reflects a worldwide shift towards renewable and sustainable energy technologies [22]. China and the United States dominate the global photovoltaic (PV) market, with installed renewable energy capacities of 760 GW and 265 GW, respectively. In Africa, the installed capacity reached approximately 221 GW, primarily consisting of hydropower plants, PV solar installations, and biomass energy sources [22].

Reduction in operational cost and improved efficiency have resulted in the increased adoption of renewable energy in standalone and grid-connected mini-grids or microgrids [23,24]. The benefits are in addition to the reduced emission of pollutants into the atmosphere during renewable energy usage [25]. For these reasons, renewable energy generation is a highly beneficial method of energy generation. This has led to an increased number of pieces of literature on renewable energy [23]. Solar PV and wind renewable energy sources are the most adopted methods of renewable energy generation [26]. Meteorological variables determine these resources; hence, they are intermittent . To improve the reliability of energy systems powered by intermittent sources, designers usually hybridize these sources [27]. Also, using energy storage devices can mitigate intermittency in renewable energy systems [28]. A well-planned and robust storage facility can be integrated into the hybrid system to further strengthen stability, efficiency, and reliability [29]. A combination of optimally designed solar PV, wind, and biomass energy sources and an improved battery storage system will enhance the operational performance and improve efficiency, reliability, and availability [30]. The system will reduce operational, emissions, and energy costs for a rural farm facility [31].

Various literature has made different contributions to hybrid renewable energy systems. For example, Babatunde et al. [17] investigated the viability of adopting an off-grid solar PV source with battery storage for a farm facility. The study addressed the issue of the energy needed for essential load-demanding equipment in a farm facility. An assessment of solar and wind energy for Sudanese agriculture was investigated by Khan et al. [32]. The analysis solely considered the energy needed to pump water for the farm. The study considered only two energy sources. Elmorshedy et al. [33] considered the potential of using a hybrid system to supply electricity for irrigation purposes. Furthermore, the energy system considered in the assessment consists of only solar PV and wind turbines. Pandyaswargo et al. [34] focused on the technical, social, and economic aspects of supplying energy for agricultural purposes for an Indonesian plantation. It considered three energy sources, which will increase the reliability of the hybrid system. Examining the viability of producing cheap electricity for a farm utilizing two energy sources, namely gas and solar power, was performed by [35]. The research suggested analyzing the system's costs. A study on solar-powered water pumping equipment for irrigation and providing drinking water to the local community was investigated by Chandel et al. [36]. The research addressed an important issue in the farm facility. Elkadeem et al. [37] worked on utilizing Dongola, Sudan, as a case study to examine the viability of a hybrid techno-economic grid system for electrifying irrigation and agricultural areas.

Grid-isolated hybrid renewable energy systems for the agricultural sector were designed and evaluated from a technological and economic perspective [38]. Research into how solar energy innovations can be used in agricultural greenhouses was performed by [39]. The research successfully addressed the critical issue of energy shortage in a farm facility. Bey et al. [40] used Algerian dairy farms as a case study to explore the possibility of deploying grid-connected PV systems for agricultural purposes, concentrating on the load demand for a livestock farm alone. Carroquino et al. [41] worked on using drip irrigation with off-grid renewable energy systems in Mediterranean agriculture. The application of a hybrid renewable energy system, simulation, and optimization for a Cuban farm was investigated by [42].

Further studies were still conducted by some other authors, Rinaldi et al. [43] investigated a combination of renewable energy systems' optimization and financial viability analysis for Peruvian rural electrification. Li et al. [44] worked on using west China as a case study, to construct an ideal and techno-economic analysis of a solar wind biomass off-grid hybrid power system for remote rural electrification. Murugaperumal et al. [45] used various operational strategies to work on the best design for a hybrid renewable energy system while employing load forecasting for rural electrification. Ahmad et al. [46] investigated using Kallar Kahar as a case study, to conduct a techno-economic analysis of a hybrid renewable energy system that combines wind, solar, and biomass for rural electrification. India's rural electrification via techno-economic hybrid renewable energy system analysis was conducted by [47]. Furthermore, adopting renewable energy in Morocco's six different temperature zones to provide energy for standard public facilities was conducted by [48]. Fodhil et al. [49] investigated the Algerian rural electrification using photovoltaic-diesel-battery through hybrid energy system while sensitivity analysis, optimization, and potentials were considered. An evaluation of the performance of a standalone PV, wind, diesel, and battery hybrid system that is suitable for a big resort complex in Malaysia's South China Sea was conducted by [50]. Also, a review of energy management in hybrid renewable energy systems and its methods was conducted by [51]. Siddaiah et al. [52] reviewed the methodologies for modeling, optimizing, designing, and configuring hybrid renewable energy systems for use in off-grid networks, and an analysis of how to make hybrid renewable energy power plants more efficient was conducted by [53]. This study describes a cutting-edge hybrid renewable energy system application in Nigeria with a focus on rural farm facilities.

The agriculture industry has seen multiple instances of the implementation of renewable energy systems. For example, since the 1970s, irrigation powered by solar energy has been used [54,55]. Its appeal has increased, as has implementation, as a result of recent advancements in distribution and finance models as well as efficiency gains. As of December 2020, India has deployed approximately 272 000 systems, leading the way in Asia [56,57]. Approximately 1500 systems have been installed in Bangladesh; by 2027, 10,000 are expected to be in place [56]. More than 40.000 solar water pumps were sold in 2019 and 2020, mostly in East Africa (mostly Kenya, Uganda, and Senegal) and India

[56]. At least 130 million solar water pumps on smallholder farms (less than 1 hectare) in West, Central, and East Africa, as well as 33 million units in South Asia, have the technical ability to be installed [56]. Millions of small farmers in Sub-Saharan Africa stand to gain from the predicted more than doubling of irrigated areas by 2050 [56,58]. Furthermore, the potential for solar water pumps to take the place of current diesel-powered or grid-connected pumps is not included in those numbers.

Contributions to knowledge

This study makes several significant contributions to the field of hybrid renewable energy systems for agricultural applications. A comprehensive comparative analysis of ten different hybrid energy system configurations is provided, offering insights into the trade-offs between various system designs for diverse agricultural contexts. The research optimizes hybrid renewable energy systems specifically for rural farm facilities in Nigeria, considering unique local energy needs, resource availability, and economic conditions. Biomass is incorporated as a key component of the hybrid system, utilizing agricultural waste as an energy source alongside solar, wind, and conventional sources in an off-grid setting. A holistic evaluation combining technical feasibility, economic viability, and environmental impact is presented, offering a comprehensive understanding of system implementation in rural agricultural settings. By focusing on a real-world case study, this research bridges the gap between theoretical models and practical application, providing actionable insights for sustainable energy solutions in rural agriculture. These contributions advance the understanding of optimal design, implementation, and management of hybrid renewable energy systems in rural agricultural settings, particularly in developing countries. The study provides a framework applicable to similar contexts worldwide, potentially transforming energy access and sustainability in rural farming communities.

Location

The farm facility used as case study for this research is the Bill and Melinda farm facility at the Federal University of Agriculture, Abeokuta, Ogun State, Nigeria. The farm facility is located within the premises of the university campus. The Bill and Melinda farm facility was used as a case study for the research because it is a standard farm with international collaboration and grants intending to add value to Africa. An aerial view of the university is shown in Fig. 1.

Load demand

There are several load demand models available in literature; however, for this study, the model defined by [59] was adopted as given in Eq. (1):

$$E_d = \sum_{f \in F} N_e \times \left(\sum_{e \in E} N_{ef} P_{ef} t_{ef} \right) \tag{1}$$

Where e is the type of equipment, i.e., refrigeration, heating, cooling, lighting, f is the class of Load (agricultural), N_e is the number of users using e type of equipment, N_{ef} is the number of types of equipment that are part of a particular class, P_{ef} is the nominal electric power rating of equipment e in class f and t_{ef} is the total duration of usage of equipment e that belongs to class f

The farm facility has several sections, such as the hatchery, cold room, incubator room, incubator boxes, hatchers room, chicks' room, brooding unit, processing unit, breeder unit, growers' unit, pasteurizing unit sections, toilets, bathrooms, and administrative blocks with offices. Each of these sections has its loads due to the electrical equipment applied for the operations of the farm facility. An energy audit was conducted during multiple site visits to assess the electrical equipment used on the farm. The audit recorded each appliance's power ratings, quantities, usage times, and durations. The load profile of the farm is depicted in Fig. 2. The load profile depicted in Fig. 2 was generated using the power rating of the different electrical equipment in the farm and their time and duration of usage over a 24-hour duration, which is expected for the farm to be operational. The total energy consumption of the farm is 1386.85 kWh/day, which amounts to 506,200.25 kWh yearly. A day-to-day random variability and time step of 5% was assumed to make the load demand more realistic. Hence, the daily load demand is estimated at 1444.52 kWh, and the annual energy demand is 527,250 kWh.

HOMER input parameters

Meteorological data

The National Space Research and Development Agency (NASRDA) provided hourly data on global solar radiation, wind speed, and temperature for the specified farm location. The meteorological data was necessary to provide the HOMER program with the energy input required to calculate the power output of the solar PV array and wind turbines at the farm facility. The data supplied the essential localized

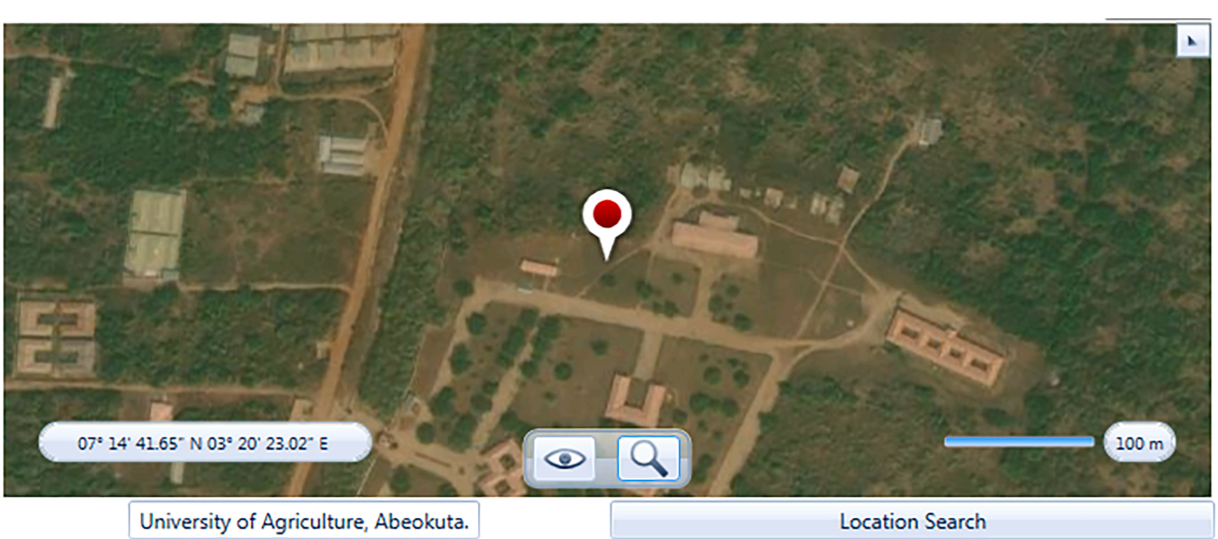

Fig. 1. Aerial view of the federal university of agriculture, abeokuta, Nigeria.

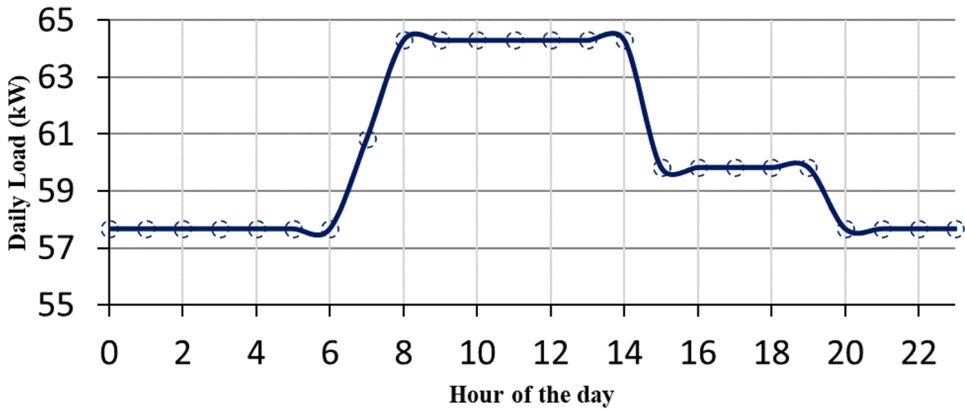

Fig. 2. Farm Load Profile.

weather measurements for the HOMER simulations.

Hybrid system economic parameters

The total life cycle cost represented by the net present cost (NPC) was required to evaluate the optimal hybrid system considering cost. The NPC accounts for all the costs of the hybrid system over its lifetime; this includes the upfront capital costs for equipment purchase and installation and ongoing operational and maintenance expenses. Significant components that contribute to the NPC are the annual maintenance and operational costs, the cost of replacing equipment after its useful lifetime, expenditure on fuel for generators, any carbon emission penalties, and expenses incurred for grid electricity usage. The NPC sums up all these present and future costs considering the time value of money. It represents the aggregated net costs adjusted for inflation and interest rates. The NPC provides a present dollar value of the overall lifecycle costs to enable an accurate economic analysis of the proposed hybrid system. The NPC is the present value of the installation and operating cost of the system over the system's lifetime minus the present value of all the income revenues earned by the project over its lifetime. The revenues are power sales from the grid and the salvage value [60]. HOMER uses Eq. (2) to estimate the total NPC of the energy systems.

$$NPC_{Total} = \frac{C_{ann,\ Total}}{CRF} \tag{2}$$

where CRF is the capital recovery factor, $C_{ann,\ Total}$ is the total annualized cost, NPC_{Total} is the total net present cost. The total annualized cost is calculated by adding the annualized costs of each system component and the other annualized cost. It is an essential value since HOMER utilizes it to compute both the levelized cost of energy and the overall net present value.

HOMER defines levelized cost of energy (COE) as the average cost per kWh of useful electrical energy generated by the system. HOMER calculates the COE by dividing the yearly cost of producing electricity (the total annualized cost) by the total useful electric energy production. The equation for the COE is given in Eq. (3) [61]:

$$COE = \frac{C_{ann,\ Total}}{E_t} \tag{3}$$

where *COE* is the cost of energy, E_t is the energy generated over time and t is the duration in years. According to [62], the capital recovery factor can be computed in relation to interest rate (i) and the project life time (n) as Eq. (4):

$$\mathrm{CRF} = \frac{i(1+i)^n}{(1+i)^n - 1} \tag{4}$$

In a PV/wind/biomass/diesel/battery hybrid system, the annualized cost of the total hybrid system can be presented as Eq. (5):

$$C_{ann,\ Total} = \sum_{N=1}^{N_{PV}} C_{ann,PV} + \sum_{N=1}^{N_{wt}} C_{ann,wt} + \sum_{N=1}^{N_{bm}} C_{ann,bm} + \sum_{N=1}^{N_{DG}} C_{ann,DG} + \sum_{N=1}^{N_{batt}} C_{ann,batt} + \sum_{N=1}^{N_{conv}} C_{ann,conv} \tag{5}$$

where $C_{ann,\ Total}$ is the total annualized cost, $C_{ann,\ PV}$ is the total annualized cost of the PV module, $C_{ann,wt}$ is the total annualized cost of the wind turbine, $C_{ann,bm}$ is the total annualized cost of the biomass gasifier, $C_{ann,DG}$ is the total annualized cost of the diesel generator, $C_{ann,batt}$ is the total annualized cost of the battery, $C_{ann,conv}$ is the total annualized cost of the converter, N_{PV} is the number of PV modules, N_{wt} is the number of wind turbine N_{bm} is the number of biomass gasifiers, N_{DG} is the number of diesel generators, N_{batt} is the number of batteries and N_{conv} is the number of converter(s)

Mathematical representation of a pv system

The energy output from the PV system varies at separate times of the day, climatic conditions of the day, and seasons of the year; this means that a good knowledge of the historical daily and seasonal weather information will be of great importance to any PV system planner to grasp the capability of the planned PV system energy output. According to Olatomiwa et al. [63], the output power of a PV system can be computed while taking into consideration the result of solar radiation and temperature as Eq. (6):

$$P_{PV-gen} = P_{mp-STC} \times \left(\frac{G}{G_{STC}}\right) \{1 + K_T(T_{cell} - T_{STC})\} \tag{6}$$

where P_{PV-gen} is the generated output power of the PV module, P_{mp-STC} is the rated module power of the PV at standard test conditions, T_{STC} is the temperature at standard test conditions, T_{cell} is the PV module cell temperature, K_T is the PV module power temperature coefficient, G is the inclined surface solar radiation in (W/m^2), G_{STC} is the solar radiation at standard test conditions which is obtained from the datasheet of the manufacturer.

From Eq. (6), T_{cell} is represented by Eq. (7):

$$T_{cell} = T_{amb} + \left\{\frac{[NOCT - 20]}{800}\right\} \times G \tag{7}$$

where T_{amb} is the ambient temperature in (°C), *NOCT* is the normal cell temperature in (°C) and it is most times stated in the datasheet of the manufacturer, G is the inclined surface solar radiation in (W/m^2), the total output power produced by the total PV panels will be the multiplication of the generated output power of the PV module (P_{PV-gen}) and the total number of PV panels (N_{PV}) to be used. This will be represented mathematically as Eq. (8):

$$P_{PV(t)} = P_{PV-gen} \times N_{PV} \tag{8}$$

where $P_{PV(t)}$ is the total output power generated by the total PV panels, P_{PV-gen} is the generated output power of each PV module, N_{PV} is the total number of PV panels.

Mathematical representation of a wind turbine system

The wind turbine transforms the energy in the wind into electrical energy. Its working principle is based on the conversion of the kinetic energy possessed by the wind in the rotor of the wind turbine for the generation of electricity. The electrical output power of a wind turbine in a wind farm depends upon certain factors such as the specification of the turbine, distribution of wind speed, the turbine conversion efficiency and it maintenance [64]. Other factors influencing the electrical power output are the tower height and the power output curve [65]. Therefore, converting wind energy to electrical energy will be maximally efficient only when designed for the particular wind farm where it will based [66]. This implies that choosing the appropriate mathematical representation is very essential in wind turbine design and simulation. . Understanding the turbine's rated power, cut-in speed, and cut-out speed is essential. Considering losses from wake effects and mechanical availability is essential [67]. The output of a wind energy system is determined by the rated speed, the turbine's power rating (P_R), the cut-out and cut-in speeds [68]. To estimate the power generated by a wind turbine system, the following equation is used [68]:

$$P_o = \begin{cases} 0 & 0 \le v\langle v_{ci} \ \ and \ v\rangle v_{co} \\ av^3 + bP_R & v_{ci} \le v < v_R \\ P_R & v_R \le v \le v_{ci} \end{cases} \tag{9a}$$

$$a = \frac{P_R}{v^3{}_R - v^3{}_{ci}} \tag{9b}$$

$$a = \frac{v^3{}_{ci}}{v^3{}_R - v^3{}_{ci}} \tag{9c}$$

where v_R, v_{ci}, and v_{co} are the wind turbine's rated, cut-in, and cut-out speeds, respectively. The height of a wind turbine can significantly impact the amount of energy generated at a given location. To account for variations in wind turbine blade height, the Power Law is commonly used [68]:

$$\left(\frac{v}{v_{ref}}\right) = \left(\frac{h}{h_{ref}}\right)^{\beta} \tag{9d}$$

Where v is the wind speed at hub height h, v_{ref} represents the wind speed measured at the reference height h_{ref} and β are the power law exponents that change with elevation, time of day, season, terrain, wind speed, and temperature.

The average electrical hourly output power of a wind turbine is measured using the wind speed measured at a predetermined height. According to Babatunde et al. [69], HOMER applies the power law, using Eqs. (9e) and (9f), the obtained numerical value at the height is normalized in accordance with the height of the hub indicated in the design.

$$V_h = V_m \left(\frac{\ln\left[\frac{H_h}{S_r}\right]}{\ln\left[\frac{H_m}{S_r}\right]} \right) \tag{9e}$$

$$V_h = V_m \left(\frac{H_h}{H_m}\right)^{\beta} \tag{9f}$$

where

V_h is the speed of the wind at the height of the hub
V_m is the speed of the wind at the height of the anemometer
$H_h$is the height of the hub
H_m is the height of anemometer
S_r is the length of the surface roughness
β is the exponent of power law

After this procedure, the wind turbine's power output is calculated by multiplying the process output under standard temperature and pressure with the air density using Eq. (9 g).

$$P_w = \frac{\rho}{\rho_o} \times P_{w-stp} \tag{9 g}$$

where

P_w is the output power of the wind turbine
ρ is the density of air
ρ_o is the density of air at standard temperature and pressure
P_{w-stp} is the output power of the wind power at standard temperature and pressure

Mathematical representation of a biomass system

Biomass can be produced through animal waste, plant waste, food waste, industrial waste, and other bio-energy resources from the forest [70]. Biomass exists in the form of biogas or bio-fuel liquid. Power is generated by the biomass gasifier so long as the feedstock is available. According to Babatunde et al. [21], the gasifier power output is mathematically represented as Eq. (10):

$$P_{bmg} = \frac{Available\ biomass\ (tons\ per\ year) \times CV_{bmg} \times \eta_{bmg} \times 1000}{365 \times Operating\ hours\ per\ day} \tag{10}$$

where P_{bmg} is the power output of the biomass gasifier, CV_{bmg} is the biomass gasifier calorific value and η_{bmg} is the efficiency of conversion of the total biomass gasifier system.

The values of plant and animal wastes were required for the case study farm. The farm waste data was obtained by a visitation to the farm facility for an on-the-spot assessment of the total waste generated hourly and daily. HOMER used these data as the energy input resources for the computation of the power output from the biomass gasifier.

Mathematical representation of a diesel generator system

An integration of a diesel generator into the hybrid system will complement the renewable energy means of electricity generation thereby increasing the reliability of the hybrid system. According to [71], the fuel consumption of a diesel generator in (litre/hour) is modeled as Eq. (11) and (12):

$$F_G = B_G \times P_{G-rated} + A_G \times P_{G-out} \tag{11}$$

$$F_G\ (litres\,/\,hour) = A_G \times P\ (kW) + B_G \times P\ N\ (kW) \tag{12}$$

where F_G is the fuel consumption of the diesel generator, $P_{G-rated}$ is the nominal power of the diesel generator, P_{G-out} is the output power of the diesel generator, P is the electrical power from the diesel generator, $P\ N$ is the rated (nominal) power of the diesel generator, A_G and B_G are the coefficients of the fuel consumption curve in (litre/kWh) defined by the user.

Mathematical representation of a battery bank storage system

When the battery is charging, this means that the power generated by the renewable energy sources is greater than the energy demand. According to [72], the battery charging capacity is represented mathematically as Eq. (13):

$$C_B(t) = C_B(t-1) \times (1-\sigma) + \left[P_T(t) - \frac{P_L(t)}{\eta_{inv}}\right] \times \eta_{Batt} \tag{13}$$

where C_B(t) is the battery charging capacity at time t, $C_B(t-1)$ is the battery charging capacity at time t minus 1 second, σ is the rate of the battery self-discharging, P_T(t) is the total power of the renewable energy sources in the hybrid system at time t, $P_L(t)$ is the total load demand power of the system at time t, η_{inv} is the efficiency of the inverter and η_{Batt} is the efficiency of the battery.

The total power of the renewable energy sources in the hybrid system at time t, (P_T(t)) is also given as Eq. (14):

$$P_T(t) = N_{PV}P_{PV} + N_{wt}P_{wt} + N_{BG}P_{BG} \tag{14}$$

where P_{PV} is the output power of the PV panel, P_{wt} is the output power of the wind turbine, P_{BG} is the output power of the biomass gasifier, N_{PV} is the number of PV modules, N_{wt} is the number of wind turbines and N_{BG} is the number of biomass gasifier

In a situation whereby the renewable energy sources generated power is lower than the load demand, the battery bank being in operation at these periods will be in the discharge state. Therefore, according to [63], the nominal capacity of the battery and the charge quantity of the battery bank at these periods can be represented as Eqs. (15) and (16) respectively

$$C_{Batt}(\mathrm{Wh}) = \frac{P_L(t) \times AD}{\eta_{Batt} \times \eta_{inv} \times DOD} \tag{15}$$

$$C_B(t) = C_B(t-1) \times (1-\sigma) + \frac{\left[\frac{P_L(t)}{\eta_{inv}} - - P_T(t)\right]}{\eta_{Batt}} \tag{16}$$

where C_{Batt}(Wh) is the nominal capacity of the battery, DOD is the depth of discharge, AD is the number of days chosen to be the day of autonomy (the number of days that the battery can supply the site loads without any form of support from any generational source), P_T(t) is the total power of the renewable energy sources in the hybrid system at time t, $P_L(t)$ is the total load demand power of the system at time t, η_{Batt} is the efficiency of the battery, η_{inv} is the efficiency of the inverter, σ is the rate of the battery self-discharging and the battery state of charge (SOC) is given by Eq. (17) [73]:

$$SOC_{min} \leq \mathrm{SOC}\ (\mathrm{t}) \leq SOC_{max} \tag{17}$$

The minimum state of charge is given as Eq. (18):

$$SOC_{min} = 1 - DOD \tag{18}$$

where SOC is the state of charge, SOC_{min} is the minimum state of charge, SOC_{max} is the maximum state of charge, DOD is the depth of discharge and the maximum DOD of a battery is between 30 and 50 % if the battery is to have a considerable maximum battery life [49].

Mathematical representation of a rectifier

In the hybrid system, when the energy generated by the renewable energy sources is greater than that of the load demand energy, the rectifier transforms the excess AC power to DC for storage in the backup system for future use. The mathematical representation for a rectifier is given as Eqs. (19) to (21) [74]:

$$E_{REC-OUT}(t) = E_{REC-IN}(t) \times \eta_{REC} \tag{19}$$

$$E_{REC-IN}(t) = E_{EXC-AC}(t) \tag{20}$$

At any particular time, t,

$$E_{EXC-AC}(t) = E_{(From\ all\ the\ eenergy\ sources)}(t) - E_{Load}(t) \tag{21}$$

where $E_{REC-OUT}(t)$ is the output of energy from the rectifier hourly, $E_{REC-IN}(t)$ is the input of energy to the rectifier hourly, $E_{EXC-AC}(t)$ is the amount of excess energy from all the sources of AC and η_{REC} is the rectifier's efficiency

Mathematical representation of an inverter

The solar PV and battery give out power in DC form, and if the hybrid system consists of AC loads, this means that there will be the need to transform DC power to AC power to energize the AC loads. This will be done using an inverter. The mathematical representation for an inverter supplying power from a solar PV and battery is given as Eqs. (22) and (23) (Gupta et al., 2011):

$$E_{PVG-INV}(t) = E_{PVG}(t) \times \eta_{INV} \tag{22}$$

$$E_{BATT-INV}(t) = \frac{E_{BATT}(t-1) - E_{Load}(t)}{\eta_{INV} \times \eta_{DCHG}} \tag{23}$$

where $E_{PVG-INV}(t)$ is the inverter energy output from the solar PV source on an hourly basis, $E_{BATT-INV}(t)$ is the inverter energy output from the battery source on an hourly basis, η_{INV} is the inverter efficiency, η_{DCHG} is the charging and discharging efficiency of the battery, $E_{Load}(t)$ is the energy used to power the load and $E_{PVG}(t)$ is the energy from the solar PV

Mathematical representation of a charge controller

The charge controller is used to regulate the amount of charge that moves from the charging source to the battery. It monitors the state of charge of the battery and detects when the battery is fully charged to cut off the supply to the battery from the charging source. Mathematically, the charge controller is represented as Eqs. (24) and (25) (Gupta et al., 2011):

$$E_{CC-OUT}(t) = E_{CC-IN}(t) \times \eta_{CC} \tag{24}$$

$$E_{CC-IN}(t) = E_{REC-OUT}(t) + E_{EXC-DC}(t) \tag{25}$$

where $E_{CC-IN}(t)$ is the energy input to the charge controller on an hourly basis, $E_{CC-OUT}(t)$ is the energy output from the charge controller on an hourly basis, $E_{EXC-DC}(t)$ is the amount of excess energy from the DC source, $E_{REC-OUT}(t)$ is the output of energy from the rectifier hourly and η_{CC} is the efficiency of the charge controller (Table 1).

Reliability analysis for the optimal operations of the hybrid energy system

In the process of the supply of energy to meet the energy demand of the consumer, occasionally, the energy generated by the hybrid system is not enough to meet the energy requirement of the consumer. This may be attributed to insufficient or total unavailability of the energy resources required to generate the energy for consumption. In such cases, there will be loss of power in varying magnitude to the consumer depending on the level of availability of the energy resources available for the generation of energy. In this study, the loss of energy probability (LOEP) and availability indices was used for the reliability evaluation of the hybrid system. According to [75], LOEP and Availability can be represented by Eqs. (26) and (27) respectively.

$$LOEP = \frac{\sum_{j=1}^{8760} Unmet_j}{\sum_{j=1}^{8760} Demand_j} \tag{26}$$

$$Availability = 1 - \left(\frac{\sum_{j=1}^{8760} Unmet_j}{\sum_{j=1}^{8760} Demand_j}\right) \tag{27}$$

where

j is time in hour

$Unmet_j$ is the total load needed by the consumer but not supplied in

Table 1
Costs and technical specifications of system components.

Item	Lifetime	Investment Cost ($)	Cost of Replacement ($)	O & M Cost ($/yr.)	Nameplate
PV	25 yrs.	137.30	135.00	2.50	0.26 kW DC
Wind Turbine	20 yrs.	971.08	971.08	29.13	1 kW
Battery	4 yrs.	364.52	364.52	10.00	12 V, 219 Ah
Biomass	15,000 hrs.	500.00	500.00	0.03	1 kW
Diesel Generator	15,000 hrs.	372.46	372.46	0.05	2.60 L/hr., 0.251 L/hr./kW
Converter	5 yrs.	121.51	121.51	10.00	1 kW
Project Life	25 yrs.				
Annu. Interest 11.5%					
Diesel Price 1.75/L					

hours of the year

$Demand_j$ is the total load demand by the consumer in hours of the year

Also, the capacity factor which is the average power output of the hybrid system divided by its nominal capacity (the ideal capacity under specified conditions of temperature and load) was considered in this research.

Assumptions, limitations and uncertainties

The capacity of the hybrid renewable energy system is expressed as

$$E_{Output} = E_{PV} + E_{WT} + E_{BG} + E_{DG} \geq E_D \tag{28}$$

where

E_{Output} is the total output energy generated by the hybrid system
E_{PV} is the total energy generated by the solar PV system
E_{WT} is the total energy generated by the wind turbine system
E_{DG} is the total energy generated by the diesel generator
E_D is total energy demand of the farm facility

The objective function of the hybrid renewable energy system is expressed as

$$Obj\ fn = mini\ (Cost + Emmission) + \max(Energy\ output) \tag{29}$$

Subject to:
Battery constraints;
Availability of resources;
Emission constraints;
Renewable energy resources operating reserve;
Balancing of power;
Shortage capacity.

Emission assessment

The environmental impact assessment of the proposed energy system begins by evaluating the fossil fuel consumption of the generator. This is used to calculate the amount of carbon dioxide (CO2) the generator emits. These calculations help estimate the CO2 emissions generated by the generator, which are then considered as the emissions avoided by using the solar PV system. The following equation can calculate the cost of environmental damage (CCO2) caused by CO2 gas [76].

$$C_{CO2} = EF_{CO2} \times E_t \times \varnothing_{CO2} \tag{30}$$

Where EF_{CO2} represents the CO_2 emission factor of the electric power generation system (kg CO_2/kWh), $\varnothing_{CO2}$ represents the carbon social cost ($/ton CO_2), which may be considered as $ 70/ton CO_2.

Several values for the CO2 emission factor are documented in literature including 3.2, 3.15, and 3.0 kg of CO2 per liter of diesel [77]. However, in this paper, an emission factor of 2.66 kg CO2 per liter of diesel is utilized to estimate the quantity of carbon dioxide [77].

Results

Technical examination of the hybrid energy system

Based on the simulation and optimization with HOMER, ten (10) possible energy systems can serve the farm facility's energy demand. The energy alternatives include EA1 (PV-Biomass-DG-battery), EA2 (PV-Wind-Biomass-DG-battery), EA3 (PV-Biomass-battery), EA4 (PV-Wind-Biomass-battery), EA5 (PV-Biomass-DG), EA6 (PV-Wind-Biomass-DG), EA7 (Biomass-DG), EA8 (Biomass-DG-battery), EA9 (Wind-Biomass-DG) and EA10 (Wind-Biomass-DG-battery). The result in Table 2 displays a series of results of the HRES system. The result indicated that the most cost-effective hybrid system combination for the farm is the integration of the PV (561.023 kW), diesel generator (88 kW), biomass (10 kW), converter (81.4005 kW), and (584) batteries (PV-Biomass-DG-battery) which were operated in a load-following mode. The result revealed that the diesel generator would have to be operational for 882 h a year and consume 12,157.9 litres of fuel. For the stated hybrid system, renewable energy was responsible for approximately 93% of the total energy generated, while the total energy generated is (795,472.9kWh/yr). The second hybrid system on the optimal ranking is the PV (571.422 kW), wind turbine (1), diesel generator (88 kW), biomass (10 kW), converter (84.9791 kW) and (573) batteries (PV-Wind-Biomass-DG-battery) which operated in the load following mode. The result revealed that the diesel generator would have to be operational for 872 h a year and consume 11,952.2 litres of fuel for the period.

The second-ranked system also contributed approximately 93% of the total energy through renewable energy means. The total energy generated for the year is (808,599.19kWh/yr). The result also revealed in the third and fourth energy alternatives that a diesel generator is not required to provide electricity. These energy alternatives operated in the cycle charging mode and the total power generated is 1540,339 and 1541,240 (kW) with renewable energy generating 100% of the total energy for the third and fourth energy alternatives respectively. The third energy alternative in the optimal ranking merged PV (1156 kW), biomass (50 kW), converter (84.3396 kW), and batteries (1246) in its energy generation. The fourth energy alternative merged PV (1156 kW), wind turbine (6), biomass (50 kW), converter (84.9901 kW), and batteries (1235) for its energy generation. The fifth energy alternative operated in the cycle charging operational mode. It merged PV (763.893 kW), diesel generator (88 kW), biomass (20 kW) and converter (80.9375 kW). The result revealed that the diesel generator would be operational for 7258 h annually and would gulp 98,098.3 litres of diesel annually. The high annual diesel consumption can be traced to the non-availability of storage battery facilities. For this period, the hybrid renewable energy system contributed only 41.5477 % of the total energy generated out of the (1328,772 kWh/yr) generated yearly. The sixth configuration utilized a cycle charging operating mode, combining multiple sources - PV array, wind turbine, diesel generator, biomass generator, and a converter. The specific capacities used were 707.057 kW for the PV array, a single 1 kW wind turbine, an 88 kW diesel generator, 20 kW biomass generator, and a 81.7587 kW converter. The

Table 2
Technical results for the different Energy Alternatives.

Rank	PV (kW)	Wind Turbine (number)	Diesel Generator (kW)	Biomass (kW)	Battery (number)	Converter (kW)	Dispatch	Diesel Generator Operating Hours (Hrs)	Diesel Generator Energy Production (kWh)	Diesel Generator Fuel (L)	Biomass (Hrs)	Biomass Energy Production (kWh)	Biomass Fuel (kg)	Renewable Fraction (%)	Energy Produced (kWh/yr)
EA1	561.023		88	10	584	81.4005	LF	882	38,394.40	12,157.90	3557	21,999.20	100.364	92.718	795,472.90
EA2	571.422	1	88	10	573	84.9791	LF	872	37,689	11,952.20	3544	22,058.20	100.375	92.8518	808,599.10
EA3	1156	-	-	50	1246	84.3396	CC	-	-	-	535	25,691.40	100.305	100	1540,339
EA4	1156	6	-	50	1235	84.9901	CC	-	-	-	534	25,713.90	100.309	100	1541,240
EA5	763.893	-	88	20	-	80.9375	CC	7258	308,189	98,098.30	2053	19,691.80	100.375	41.5477	1328,772
EA6	707.057	1	88	20	-	81.7587	CC	7443	313,452	99,947.40	2076	19,498.20	100.375	40.5496	1259,517
EA7	-	-	88	10	-	-	CC	8760	508,712	152,749	4380	18,538.20	100.375	3.51601	527,249.80
EA8	-	-	88	10	1	0.15625	LF	8760	508,710	152,749	4380	18,538.20	100.375	3.51636	527,247.90
EA9	-	2	88	10	-	0.15625	CC	8760	508,502	152,697	4380	18,538.20	100.375	3.55575	527,332.90
EA10	–	2	88	10	1	0.29583	LF	8760	508,441	152,681	4380	18,538.20	100.375	3.5674	527,271.50

LF is Load following.

simulation results showed the diesel generator operating for 7443 h annually, consuming 99,947.40 litres of diesel fuel during this runtime. This operating strategy takes advantage of the complementary nature of the different resources by charging batteries as needed to meet the load demand. The various components work together in a cycled manner based on availability and demand to optimize the system performance and economics.

Also, the sixth energy alternative contributed 40.5496 % through renewable energy out of the total (1259,517 kWh/yr) energy generated in a year. The seventh energy alternative which operated in a cycle charging operational mode merged diesel generator (88 kW) and biomass 10 (kW). This energy alternative will be operational for 8760 h in a year and consume a total of 152,749 litres of diesel for the year. 3.51601 % of the total energy generated of 527,249.80 kWh/yr was derived through renewable energy means. The eighth energy alternative is the combination of a diesel generator (88 kW), biomass (10 kW), converter (0.15625 kW), 1 battery, and operating in a load following operational mode. The diesel generator will be operational for 8760 h in a year consuming 152,749 litres of diesel. 3.51636 % of the total energy of 527,247.90 kWh/yr will be generated through renewable energy. The ninth energy alternative is the combination wind turbine (2), diesel generator (88 kW), biomass (10 kW), and converter (0.15625 kW) operating in the charge cycling mode. The diesel generator is operational for 8760 h a year and consumes 152,697 litres of diesel a year. 3.55575 % of the total generated energy of 527,332.90 kWh/yr is through renewable energy. The tenth energy alternative is a combination of wind turbine (2), diesel generator (88 kW), biomass (10 kW), and converter (0.29583 kW) in a load following operational mode. The diesel generator is operational for 8760 h annually, consuming a total of 152,681 litres of diesel. 3.5674 % of the total energy generated is through renewable energy means and the total energy generated for this energy alternative annually is 527,271.50 kWh/yr. Fig. 2 represents the hybrid configuration of the renewable energy system (Fig. 2a).

CC is cycle chargingFig. 3(a) represents the graph of the power generated by the PV cells in kilowatts against the hours of the year. It can be observed that from 0 to 2998 h, which represents the months of January to April of the year, there was almost no dip in the graph. This is because this period represents the year's dry season in Nigeria when the sun's intensity is high. This shows that there was a more stable power generation in the system; hence the use of diesel generators was discouraged during this period. From 2998 h, the dips were beginning to be noticed in the graph. This is because the rainy season starts at this period in Nigeria. The dip became more and more noticeable from 3997 h, which represents the month of May. The dips increased their frequency and decreased until 7993 h, which represents the month of November. The dips reduced drastically beyond 7993 h and a more stable power generation was observed during this period. This is because this period represents the beginning of the dry season with stable sunlight and electricity in Nigeria.

Fig. 3(b) represents the graph of the power output of the diesel generator in kilowatts against the hours of the year. The graph indicated a few spikes from 0 to 3997 h, representing the periods of January to May of the year. The result implies that the usage of diesel generators was highly reduced during this period. This is because of the efficiency of the system within this period and the availability of sunlight due to the dry season. Between the periods of 3997 and 7993 h which represents the periods of May to November of the year, there was an increase in the frequency of the spikes in the graphical result due to increased usage of the diesel generator as a result of decreased intensity of sunlight due to the rainy season. This increase in spikes increased in frequency to a point and began to decrease. Beyond 7993 h, the spikes in the graph reduced drastically due to the beginning of the dry season hence the drastic reduction in the usage of the diesel generator.

Fig. 3(c) represents the graph of the battery energy consumption in kWh against the hours of the year. From the graphical result, it can be noticed that there were a few dips between 0 and 3997 h, which

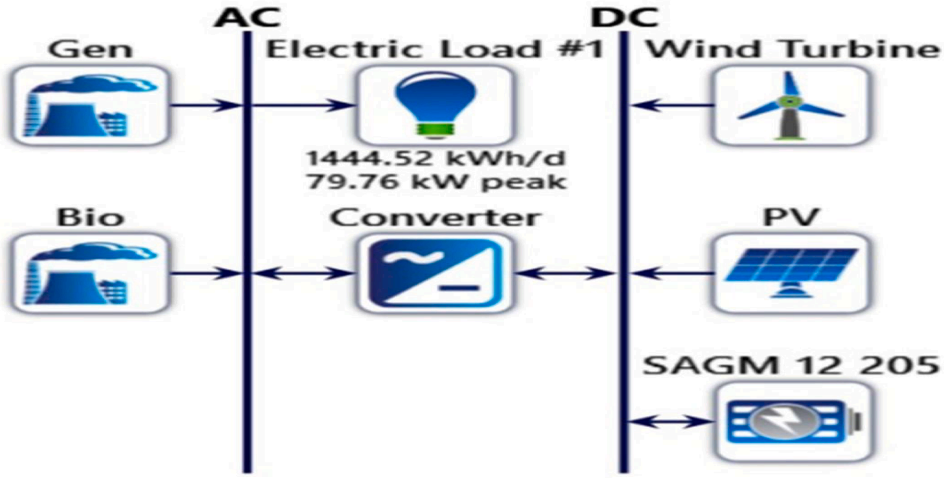

Fig. 2a. Schematic Diagram of the HRES design used for the Analysis.

represents a period between January and May of the year. This is due to the availability of more renewable energy resources that drastically reduce the use of stored energy. This resulted in a more stable and efficient system that discourages using diesel generators. Between 3997 and 7993 h, representing the months of May and November of the year, the graphical result depicted an increase in the frequency of dips to a point before a decrease was observed. This was due to the reduction in the availability of renewable energy resources as a result of the rainy season which resulted in an increase and decrease in stored energy usage. Beyond 7993 h, there was a drastic reduction in the dips witnessed in the graphical result. This was due to the resumption of the dry season and the increase in the availability of renewable energy resources, reducing reliance on the stored energy.

Fig. 3(d) represents the graph of the battery's state of charge in percentages against the hours of the year. It will be observed from the graphical result that between 0 and 3997 h i.e. the months of January to May in the year, the dips in the result were scarce which signifies the availability of renewable energy resources and less dependence on the battery's stored energy. Between 3997 and 6994 h, which represents a period between May and September, there were increased dips in the graphical result which implies increased dependence on the battery stored energy and a reduction in the number of dips between 6994 and 7993 h i.e., between the months September and November which implies a reduction in the reliance of the battery's stored energy. Beyond 7993 h, there were no dips and less dependence on the battery storage which implies the availability of renewable energy resources and no reliance on the battery storage system for its stored energy.

Table 3 represents the percentage of electricity generated by each energy component of the different energy alternatives. The result reveals that the EA1 generated 92.4% of its electricity through PV means and 2.77 % through biomass, while 4.83% was generated through diesel generators. EA2 generated 92.6 % of its electricity through PV, 2.73% via biomass and 0.0181 % through wind. 4.66 % was generated through a diesel generator. EA3 generated 98.3 % of electricity through PV and 1.67 % via biomass. EA4 generated 98.3 % through PV, 1.67 % through biomass, and 0.057% via wind. EA5 generated 75.3 % through PV, 1.48 % through biomass, and 23.2 via diesel generators. In EA6, 73.6% of its electricity was generated through PV, 1.55% through biomass, 0.0116% through wind, and 24.9% through diesel generators. Energy systems EA7 and EA8 generated their electricity through 3.52% biomass and 96.5% diesel generator, while EA9 and EA10 generated their electricity through 3.52% biomass, 0.0555% wind, and 96.4% diesel generators.

Economic examination of the hybrid energy system

Table 4 presents the economic results of the different energy alternatives. The result revealed that the EA7 has the lowest initial capital investment of $37,776.48, with seventh position in the ranking of energy alternatives. This means that the (Biomass-DG) energy combination will be easier to purchase as against the optimal system EA1 of (PV-Biomass-DG-battery) energy combination that has an initial capital investment of $556,810.3 with a difference of $519,033.82. Notwithstanding, when the operating cost of EA1, $65,713.23, was compared to the operating cost of EA7 $212,027.4, a margin of $146,314.17 was observed to be saved, giving more credence to the optimal system EA1. Furthermore, when the cost of energy (COE) of EA1 0.206325 $/kWh is compared to EA7 0.407681 $/kWh, a difference of $0.201356 will be saved for every kWh. When a comparison of the net present cost (NPC) which is the value at present of the lifetime total cost of installation and operation of the hybrid system minus the value at present of the lifetime total revenue generated/saved by the hybrid system is performed, it reveals that the optimal system EA1 had an NPC value of $1406,319 while the EA7 had an NPC value of $2778,764 with a difference $1372,445 saved over the lifetime of the hybrid system when the two energy alternatives were compared. Also, the EA1 optimal system has the lowest NPC value of all the energy alternatives.

Fig. 4 presents the breakdown of the NPC by system components. The optimal system EA1 was considered because it is the most viable and cost-effective of all the energy alternatives. Out of the total NPC of $1406,319.20, the generator contributed a fraction with the sum of $248,354.14; the PV contributed the sum of $399,999.91 while the biomass, converter, and battery components contributed $31,556.54, $40,780.85 and $719,627.76 respectively. In terms of the cost type contribution to the NPC presented in Fig. 5, the initial capital had the highest $556,810.23 which represents 39% of the total NPC; this was followed by the replacement cost of $480,300.06 which represents 34% of the total NPC value. Other cost types that contributed to the NPC are the operation and maintenance (O&M), fuel, and salvage value with the sum of $219,720.64 (15%), $157,170.88 (11%) and − $7682.60 (−1%) respectively. A clear observation of the NPC contributions in terms of cost type will reveal that after the initial capital investment of $556,810.23 which represents 39% of the total NPC, the next on the rank is the replacement cost with $480,300.06 which represents 34% of the total NPC. The replacement cost is high compared to the fuel cost of $157,170.88 (11%) because the hybrid system is powered majorly through renewable energy means, and the battery must be changed at intervals due to storage capacity degradation. Fig. 4 shows the contribution of each of the cost sections to the NPC.

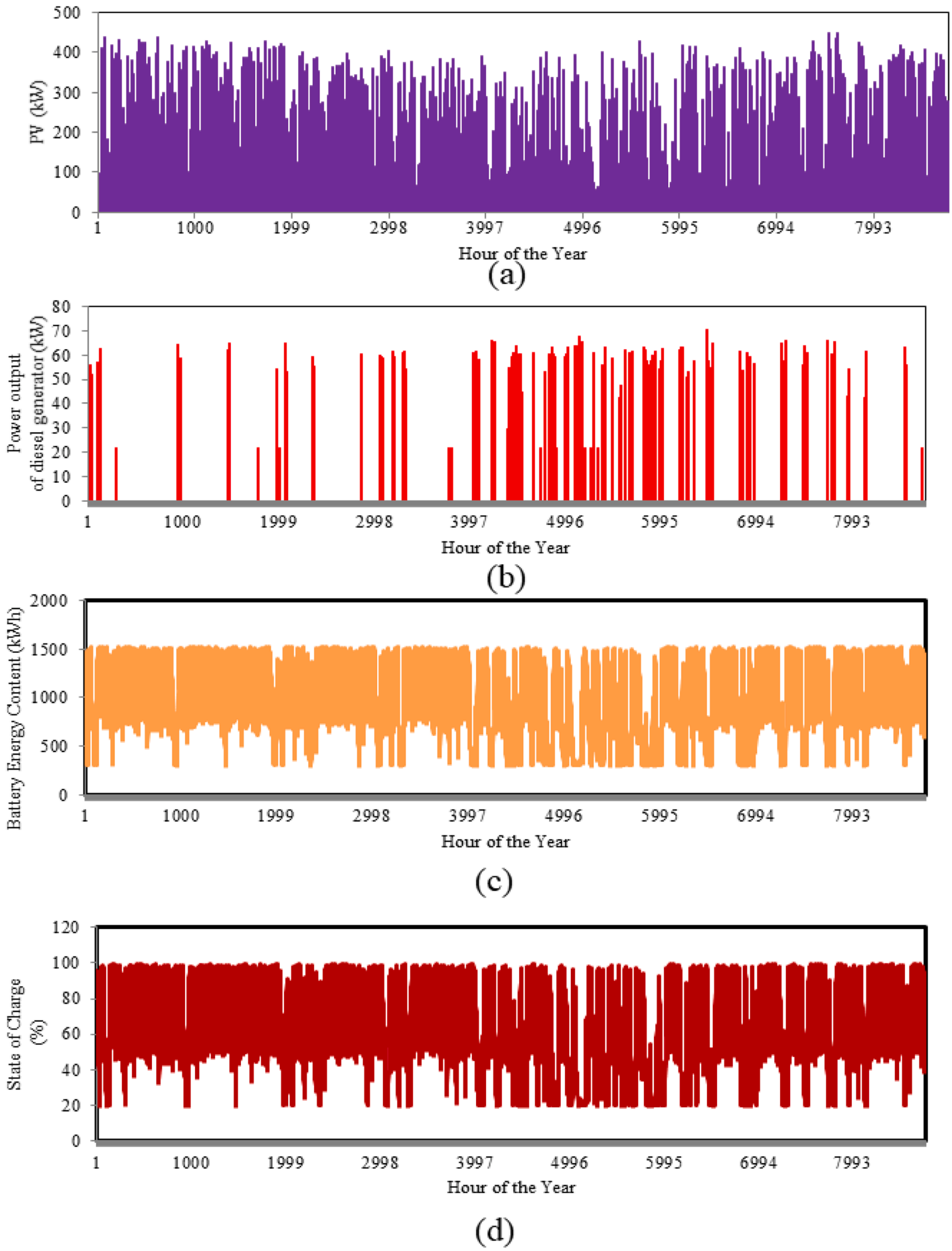

Fig. 3. Yearly PV and Diesel generator output, Battery energy content, and State of Charge.

Cash flow result

The chart result of Fig. 5 shows the cash flow of the optimal hybrid system. The result revealed a huge negative sign at the beginning of the cash flow result. This is because of the high value of the initial capital cost of the hybrid system. The second fairly high negative sign in the graph is the replacement cost. The first replacement cost was performed in the sixth year. This was a result of the degradation in some of the components of the hybrid system such as the batteries. The operational cost is another negative sign in the graph. This is due to the costs incurred due to operating the hybrid system, such as the cost of repairs and maintenance due to the hybrid system's degradation with time. Further negative sign in the graph is the fuel cost, which is minimal compared to the other negative signs. It is the cost incurred in the purchase of diesel in the running of the diesel generator.

Table 3
Percentage of Electricity Generated by each of the Energy Components Annually.

Energy Alternatives	PV (%)	Biomass (%)	Wind Turbine (%)	Diesel Generator (%)
EA1	92.4	2.77	–	4.83
EA2	92.6	2.73	0.0181	4.66
EA3	98.3	1.67	–	–
EA4	98.3	1.67	0.057	–
EA5	75.3	1.48	–	23.2
EA6	73.6	1.55	0.0116	24.9
EA7	–	3.52	–	96.5
EA8	–	3.52	–	96.5
EA9	–	3.52	0.0555	96.4
EA10	–	3.52	0.0555	96.4

Table 4
Economic results for the different Energy Alternatives.

Rank	COE ($ / kWh)	NPC ($)	Operating cost ($)	Initial capital ($)
EA1	0.206325	1406,319	65,713.23	556,810.3
EA2	0.206694	1408,833	65,684.27	559,698.3
EA3	0.260955	1777,329	52,402.34	1099,897
EA4	0.261729	1782,602	52,663.6	1101,793
EA5	0.364137	2481,971	156,717.3	456,005.6
EA6	0.36488	2487,035	159,347.9	427,062.6
EA7	0.407681	2778,764	212,027.4	37,776.48
EA8	0.407751	2779,245	212,034.9	38,159.98
EA9	0.408028	2781,128	212,058.5	39,737.63
EA10	0.408072	2781,433	212,052.6	40,119.11

Economic profitability

The result in Table 5 presents the metrics comparison of the energy alternatives. The Table revealed that the energy alternatives EA8 to EA10 present worth, annual worth, and return on investment are all negative values. This means that it is suggested not to embark on such energy alternative combinations due to foreseeable losses. EA7 combination if embarked upon, will just be worthwhile. This means that there will neither be gain nor loss. EA1 to EA6 presented various magnitudes of metrics of its present worth, annual worth, return on investment, simple payback period, and discounted payback period. The result indicated that the metrics for the present worth, annual worth, return on investment, and internal rate of return appeared in increasing order from EA6 to EA1, i.e., as it tended toward the optimal energy alternative. The simple payback period metrics increased from EA1 to EA6 between 2.97 years to 6.99 years. The discounted payback period metrics appeared in increasing order from EA1 to EA5 between 3.32 years to 10.37 years. It decreased from 10.37 years in EA5 to 9.98 years in EA6.

Environmental analysis of the energy system

The annual carbon dioxide production for each of the energy alternatives is presented in the graph of Fig. 6.

The annual carbon dioxide production in kilogram per year (kg/yr.) for all the energy alternatives ranges from 15.8 kg minimum to 399,855 kg maximum annually. It can be observed from Fig. 6 that, energy alternatives EA 7 to EA 10 produced the highest quantities of carbon dioxide at 399,855 kg, 399,854 kg, 399,717 kg, and 399,677 kg respectively. The optimal system EA1 had a fair carbon dioxide production at 31,840 kg annually. The same applies to the second most optimal energy alternative i.e., EA2 with a carbon dioxide production level of 31,302 kg annually. Energy systems EA3 and EA4 had the lowest carbon dioxide production levels of 15.8 kg annually, respectively. This makes EA3 and EA4 the most environmentally efficient and the best energy alternative for an environmentally conscious energy designer. The EA5 and EA6 produced 256,799 kg and 261,640 kg respectively.

From Table 6, a further comparison of other emissions of all the energy alternatives reveals that they follow the same graphical pattern of the carbon dioxide emission with EA3 and EA4 having the least emissions for all the different emissions compared.

Reliability analysis for optimal operations of the energy alternatives

The reliability result for the study is presented in Table 7; the table shows the annual unmet load, the annual energy demand, LOEP, and the availability of all the energy alternatives. The annual unmet load and the annual energy demand are obtained from the simulation and the load analysis respectively. The result revealed that aside from EA3 and EA4 that has LOEP of 0.000756 respectively, the remaining EAs have 0 LOEP. Also, the availability for all the EAs is 1 except for EA3 and EA4 that has an availability of 0.999244 respectively. The result shows that all the energy alternatives are highly reliable.

The variability of the hybrid energy system to change in input parameters

This study performed different variability analyses to assess the effect of the fluctuations in the output variable when it is subjected to changes in the input variables. The study performed the variability analysis of the quantity of biomass, load, diesel price, and discount rate. The result of the analysis will be discussed below.

Effect of the fluctuation in the quantity of biomass

The assessment of how the change in the quantity of biomass affects the NPC and COE was performed using the base value of 0.275 tonne per day drawn from the farm, a minimum value of 0.1925 tonne per day,

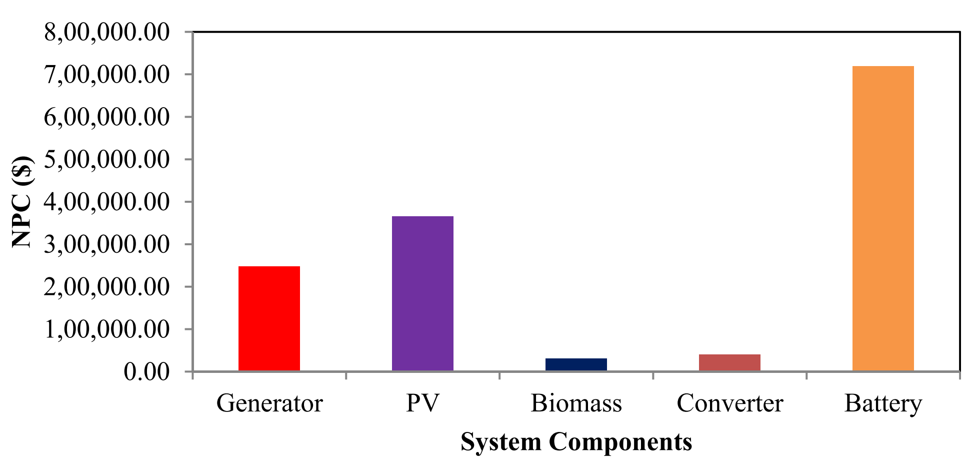

Fig. 4. Breakdown of NPC by Optimal System Components.

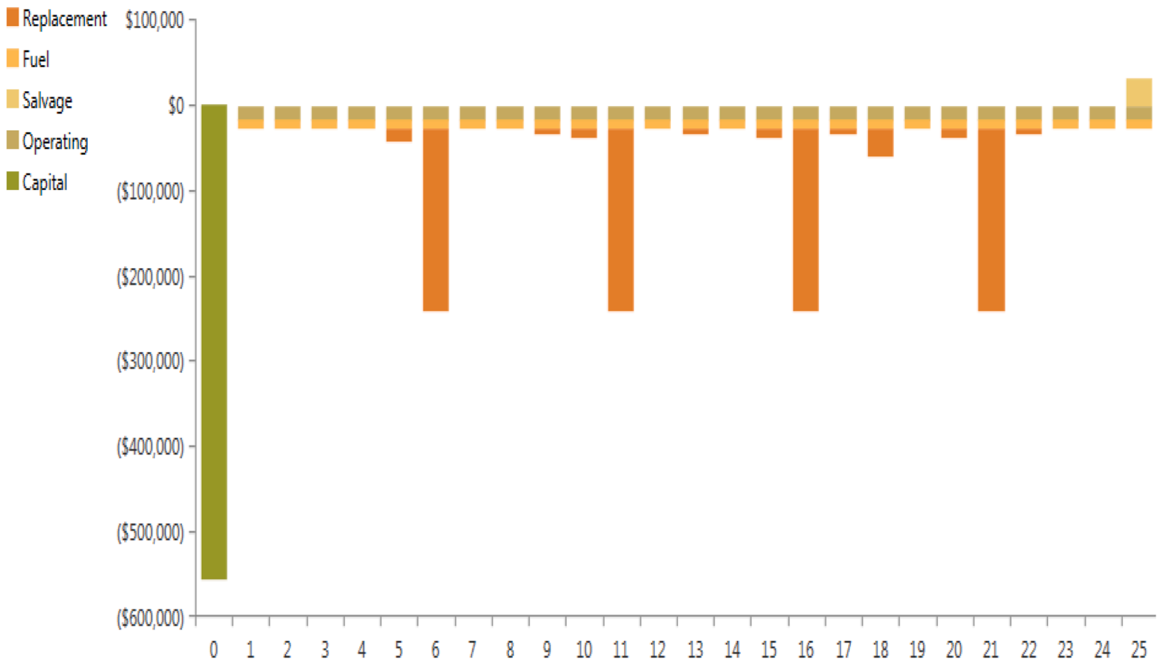

Fig. 5. Chart of Cash Flow for Optimal System.

Table 5
Economic Viability Comparison of the Energy Alternatives.

Metric	EA 1	EA 2	EA 3	EA 4	EA 5	EA 6	EA7*	EA 8	EA 9	**EA 10**
Present Worth ($)	1372,444	1369,931	1001,435	996,161	296,793	291,729	0	−482	−2364	−2364
Annual Worth ($/yr)	128,569	128,334	93,813	93,319	27,803	27,329	0	−45	−221	−221
Return on investment (%)	28.1	28	15	14.9	13.2	13.5	0	0	−1.5	−1.5
Internal Rate of Return (%)	30.8	29.7	15.2	15.2	12.7	13.1	n/a	n/a	n/a	n/a
Simple Payback (yr)	2.97	2.99	5.82	5.84	7.3	6.99	n/a	n/a	n/a	n/a
Discounted payback (yr)	3.32	3.33	7.2	7.22	10.37	9.98	n/a	n/a	n/a	n/a

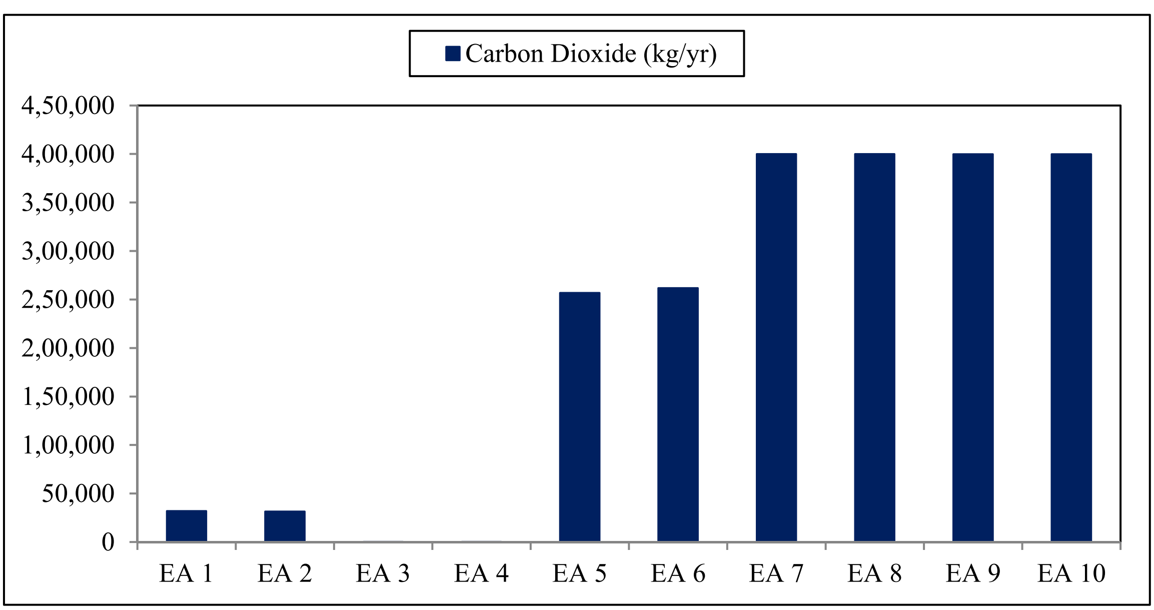

Fig. 6. Chart of Carbon Dioxide Production for the Energy Alternatives.

and a maximum value of 0.3575 tonne per day. The result is presented in Fig. 7. The result shows a relationship between the NPC and COE against the quantity of biomass used. When the quantity of biomass produced was at minimum value, the value of NPC and COE was at the highest values, and these values decreased as the quantity of biomass increased. The lowest NPC and COE were obtained when the quantity of biomass

Table 6
Emission Comparison of the Energy Alternatives.

Emissions	EA 1	EA 2	EA 3	EA 4	EA 5	EA 6	EA 7	EA 8	EA 9	EA 10
Carbon Monoxide (kg/yr)	202	199	1.64	1.64	1620	1651	2522	2522	2521	2521
Unburned Hydrocarbons (kg/yr)	8.83	8.68	0.0722	0.0722	70.7	72	110	110	110	110
Particulate Matter (kg/yr)	1.23	1.21	0.0098	0.0098	9.82	10	15.3	15.3	15.3	15.3
Sulfur Dioxide (kg/yr)	77.9	76.6	0	0	629	641	979	979	979	979
Nitrogen Oxides (kg/yr)	190	187	1.54	1.54	1522	1551	2369	2369	2368	2368

Table 7
Reliability results for the different Energy Alternatives.

	EA1	EA2	EA3	EA4	EA5	EA6	EA7	EA8	EA9	EA10
Unmet Load (kWh/yr.)	0	0	399	399	0	0	0	0	0	0
Energy Demand (Served) (kWh/yr.)	527,250	527,250	526,850	526,851	527,250	527,250	527,250	527,250	527,250	527,250
LOEP	0	0	0.000757	0.000757	0	0	0	0	0	0
Availability	1	1	0.999243	0.999243	1	1	1	1	1	1

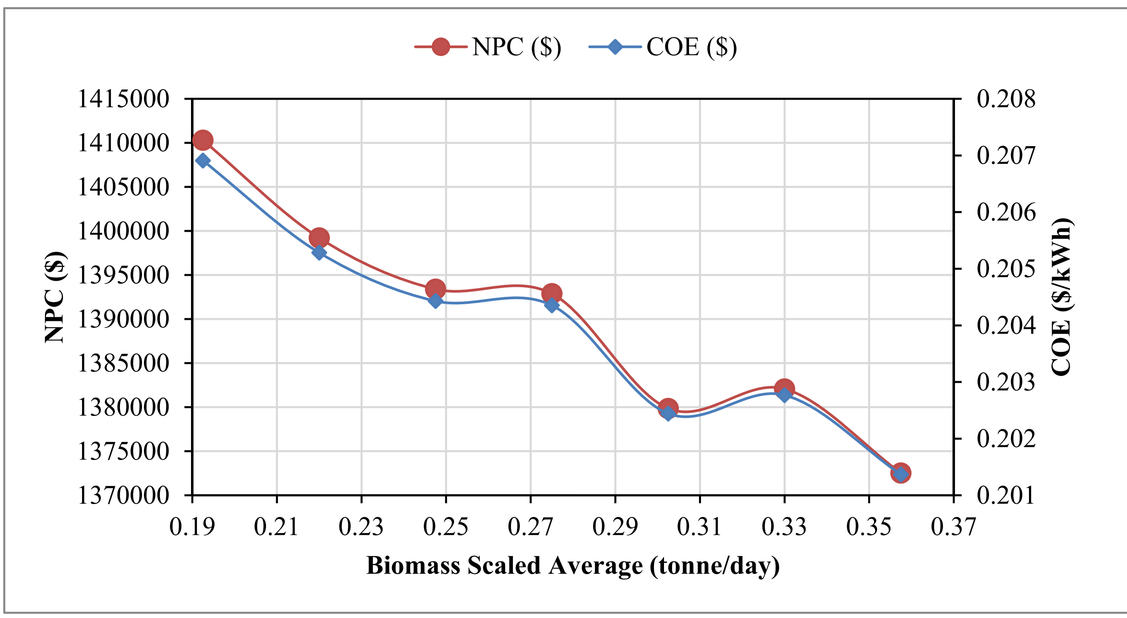

Fig. 7. Variability Result of the Change in Quantity of Biomass.

was at a maximum. The sensitivity to biomass quantity fluctuations (Fig. 7) demonstrates the system's adaptability to different farm types and resource availabilities. As biomass quantity increased from 0.1925 to 0.3575 tonnes per day, both NPC and COE decreased. This implies that farms with higher biomass production (e.g., livestock farms or those with significant crop residues) could achieve more cost-effective implementations. Conversely, farms with limited biomass resources might need to rely more heavily on other renewable sources or consider alternative configurations.

Effect of the fluctuation in the energy demand

An assessment of how the change in energy demand affects the NPC and COE was conducted. The evaluation was performed using a base value of 1445 kWh per day with a minimum value of 1145 kWh per day and a maximum value of 1745 kWh per day. The result of Fig. 8 is obtained. The result presents the NPC and COE against the energy demand. The result shows that for the NPC, the lowest value was obtained when the energy demand was at a minimum. There is an increase in the NPC as the energy demand increases but at a slow rate. This is because the NPC is made up of different costs such as the initial cost, annual operations and maintenance cost, replacement cost, fuel cost, emission penalties, and the grid power usage cost. The NPC is at maximum when the energy demand is at a maximum. For the COE, the maximum value occurs when the energy demand is at the minimum and tends to increase at a faster rate than the reduction rate of the NPC when the energy demand increases. At maximum energy demand, the COE is at a minimum value. The analysis of fluctuations in energy demand (Fig. 8) directly relates to farm size scalability. As energy demand increased from 1145 kWh/day to 1745 kWh/day, we observed that the Net Present Cost (NPC) increased at a slower rate than the reduction in the Cost of Energy (COE). This suggests that larger farms with higher energy demands may benefit from economies of scale, potentially achieving lower per-unit energy costs. However, the increasing NPC indicates that initial capital requirements would be higher for larger installations, which could be a barrier for some farm operations.

Effect of the fluctuation in the diesel price

Further assessment was performed to ascertain the effect of change in the price of diesel on the NPC and COE. The assessment was performed using a base value of $1.75 per litre with a minimum value of

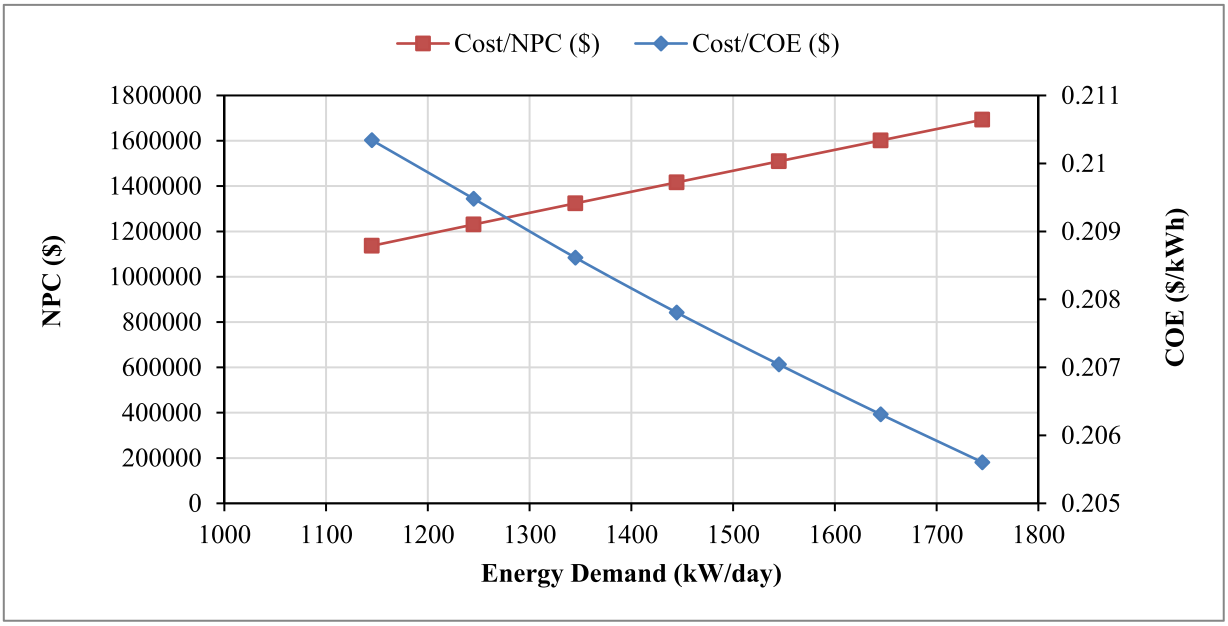

Fig. 8. Variability Result of the Change in Energy Demand.

$1.00 per litre and a maximum value of $2.50 per litre, the result of Fig. 9 is obtained. The result shows that both NPC and COE have different values of minimum at minimum diesel cost of $1.00 per litre. Both the NPC and COE tend to increase at a fast rate as the diesel price increases and have their maximum values at the maximum value of the diesel price.

The analysis of diesel price (Fig. 9) and discount rate (Fig. 10) fluctuations provides insights into the economic adaptability of the system across different contexts. The system's sensitivity to diesel prices suggests that farms in areas with high or volatile fuel costs might find greater value in maximizing the renewable energy fraction of their system. The discount rate analysis indicates that the economic viability of these systems can vary significantly based on financial conditions, which could affect scalability in different economic environments.

Effect of the fluctuation in the discount rate

The effect of the change in discount rate on the NPC and COE was performed. The base value is 14% with a minimum value of 8% and a maximum value of 20% entered into the program. The result of Fig. 10 is obtained. From the result, for the NPC, at the minimum discount rate, the NPC is at maximum and tends to decrease at a slow rate as the discount rate increases. The NPC is at a minimum at the maximum discount rate. For the COE, at the minimum discount rate, the COE is at a minimum. It tends to increase as the discount rate increases and is at a maximum at the maximum discount rate.

While not explicitly analyzed sensitivity assessment, the results suggest potential for modular scaling. The relatively linear relationships observed in most sensitivity analyses imply that system components could be added or scaled in a modular fashion to meet varying energy demands, allowing for flexible implementation across different farm sizes. Furthermore, the analysis also hints at potential limits to

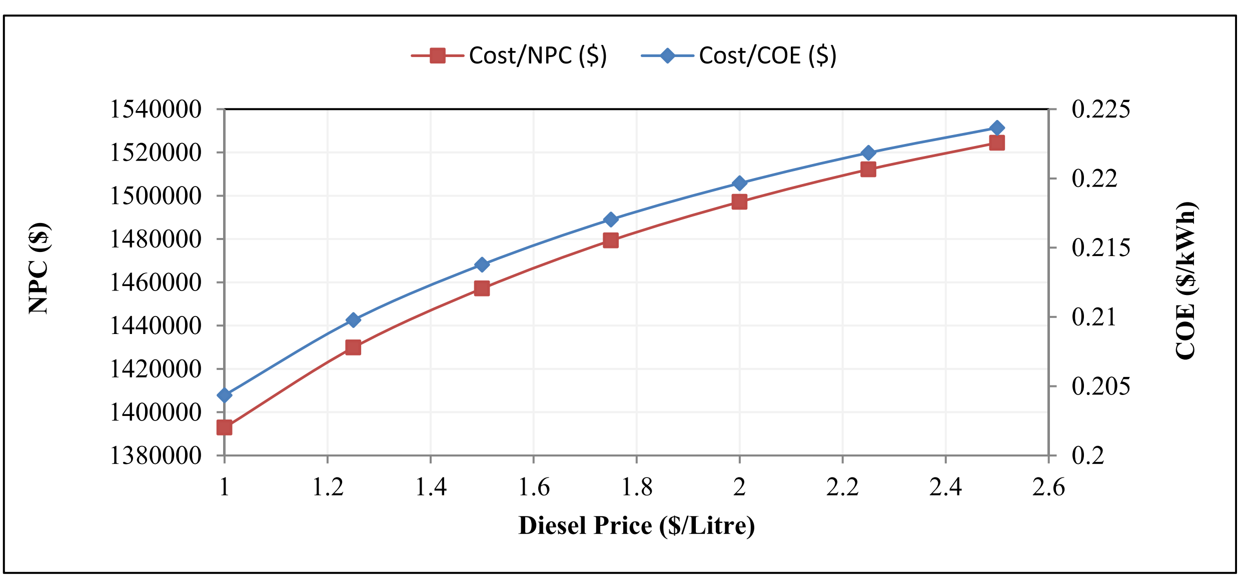

Fig. 9. Variability Result of the Change in Diesel Price.

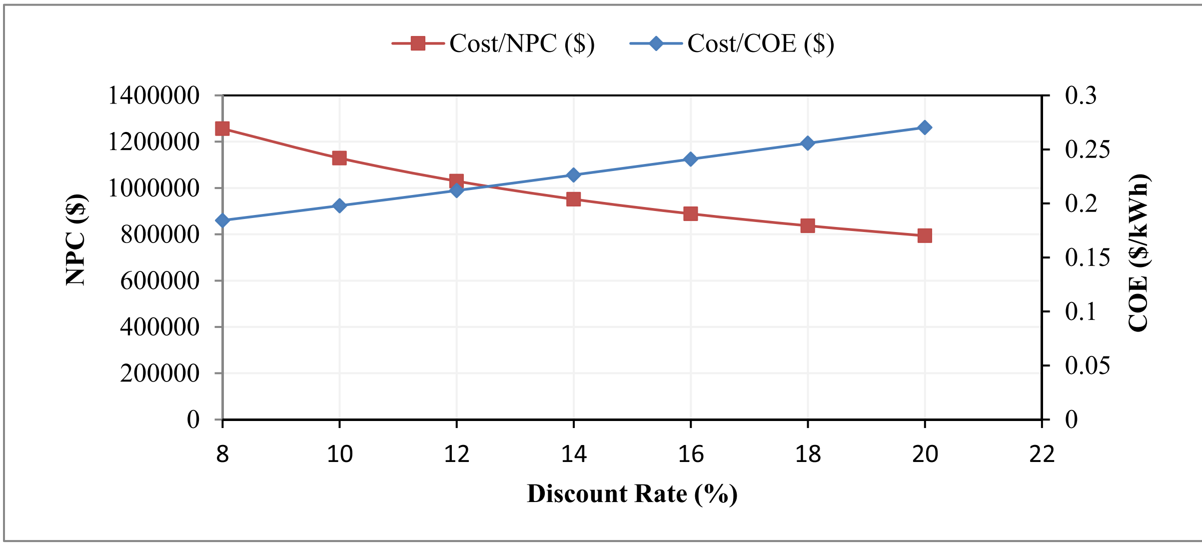

Fig. 10. Variability Result of the Change in Discount Rate.

scalability and adaptability. For instance, the diminishing returns in COE reduction as energy demand increases suggest that there may be an optimal scale beyond which further size increases yield minimal additional benefits. While this study focuses specifically on a farm facility in rural Nigeria, the methodology and findings have broader applicability to other sites and locations, particularly in developing countries with similar agricultural and energy contexts. The comprehensive analysis of multiple energy alternatives provides a framework that can be adapted to various geographical and climatic conditions.

Technical challenges and implementation barriers

This study was associated with several challenges and barriers. Some of these challenges include obtaining the required permission to access the research facility under the case study, data privacy, availability of the required data, bureaucratic processes in obtaining the required data, the time spent in obtaining the data, the cost of logistics, the project scope, and time management. Having highlighted the aforementioned, a thorough and detailed project plan was carried out to overcome the highlighted challenges. Also, a comprehensive risk assessment was performed to mitigate the effect of technical, cost and environmental risks involved during the acquisition of the required data for the study. Major stakeholders were adequately briefed during the cause of this process to avoid unnecessary conflicts and to also uphold the integrity of the obtained data. Furthermore, a rigorous and continuous monitoring of the processes were performed during the study to obtain the data with high level integrity that was used for the study. All these measures were adopted to overcome the technical challenges and barriers encounted during the study and its implementation.

Conclusions

The simulation and analysis of the results of a standalone hybrid renewable energy system for a typical rural farm facility that is not connected to the grid system was presented. The work considered a hybrid system comprising solar, biomass, wind, and diesel generator components and their resources at different times a year for a typical farm facility. The research performed simulation and analysis of various parameters of the hybrid system to give a relational output result for electricity generation for a farm facility located in the university. The energy demand of a standard farm facility in the university has been adopted for the simulation and analysis of a typical farm energy system. The total energy demand of each of the different appliances in kWh for a 24-hour period of the farm facility was obtained while considering their respective duration of usage. By this method, the foundation for the real-time energy consumption pattern of the farm has been laid. The farm's biomass energy capacity has been mathematically analyzed based on the daily production of biomass on the farm. Also, the potential of solar and wind energy for the farm has been mathematically analyzed based on the available long-term hourly and daily meteorological data. This led to the initiation of the optimal sizing and planning of the hybrid energy system for the farm facility.

The study presented an analysis of technical, economic, and environmental results obtained from the system simulation. The technical analysis revealed the most optimal system and their ranking order, the electricity generated by each component, the battery state of charge, and the battery energy content. The economic analysis revealed the ranking of the energy alternatives in terms of their respective COE, NPC, operating cost, and initial capital cost. It also presented the breakdown of NPC by the system components and the contribution of each type of cost to the NPC. Furthermore, it presented the cash flow result, economic profitability, present worth, annual worth, return on investment, internal rate of return, simple payback, and discounted payback. The environmental analysis presented the carbon dioxide production level of each of the energy alternatives, the carbon monoxide emission, the unburned hydrocarbon, sulphur dioxide, and nitrogen oxide.

The major finding in the study is as follows:

- The study shows that the optimal energy alternative for the farm facility used for the study in terms of NPC and COE in their order of ranking is EA1 PV/biomass/diesel generator/battery, EA2 PV/biomass/wind/diesel generator/battery, EA3 PV/biomass/battery, EA4 PV/biomass/wind/battery, EA5 PV/biomass/diesel generator/battery, EA6 PV/biomass/wind/diesel generator/battery, EA7 Biomass/diesel generator/battery, EA8 Biomass/diesel generator/battery, EA9 Biomass/wind/diesel generator/battery and EA10 Biomass/wind/diesel generator/battery.
- For the researched farm, EA1 is the best for NPC and COE. Energy alternatives 1 to 6 out of the 10 energy alternatives considered in this study generated significant electricity through the solar energy conversion process. It shows that energy alternatives 3 and 4 have the highest energy generation through the solar medium with a 98.3% energy contribution to the hybrid system. This suggests that the farm site considered for this investigation possesses enormous solar energy potential with the ability for solar energy applications. The biomass component contributed to all the energy alternatives as

a means of energy generation. The optimal energy alternative generates 2.77% of energy through biomass. This value decreased as the ranking decreased until energy alternative 6. It increased to 3.52% for energy alternatives 7 to 10. This disparity is a result of fluctuation in the production of the biomass resource on the farm.

- The research reveals that energy alternative 4 has the highest percentage of energy generation through the wind component, 0.057%, for the site. Energy alternatives 9 and 10 came second with 0.0555% contribution through the wind energy medium. The least energy generation through wind is energy alternative 2 with 0.0181%. The variation in the wind percentage contribution is a result of the fluctuations in the wind power. Also, the study shows that very little amount of energy is generated through wind compared to other renewable energy sources.
- The study reveals that the diesel generator improved the reliability of the hybrid system. It provided backup to the hybrid system averting power loss to the farm. It also prevented the battery from exceeding the minimum depth of discharge of 30% that was used for this study which suggested that it is highly possible to accomplish a totally off-grid energy system. The research reveals that the farm facility's enormous solar resources and good biomass production level will be the ideal hybrid renewable energy configuration for a farm in the chosen location. The renewable energy fraction can be improved if the biomass production level is increased.
- The economic breakdown of the study reveals that EA1 has the lowest COE, NPC, and operating costs. This is due to the high renewable energy fraction generation percentage. This means that electricity is produced with the barest minimum cost for diesel purchase. However, this energy alternative has the highest initial capital cost due to the high cost of purchasing and installing renewable energy equipment. Furthermore, the present worth, annual worth, return on investment, and internal rate of return of EA1 are the highest, making it the most viable. While its simple payback and discounted payback are the lowest. This makes it the most suggested energy alternative.
- Environmental analysis shows that EA1 emitted a CO_2 of 31,840 kg annually and EA2 emitted 31,302 kg annually. EA3 and EA4 had the lowest carbon dioxide production levels of 15.8 kg annually, respectively. The values increased to 256,799 kg and 261,640 kg annually for EA5 and EA6 respectively. From EA7 to EA10 it maintained a constant value of 399,677 kg annually. This makes EA3 and EA4 the most environmentally efficient among the energy alternatives and the best energy alternatives for an environmentally conscious designer.
- Variability analysis revealed that NPC and COE decrease as the quantity of biomass increases for biomass variability. For the variability of energy demand, the NPC is at minimum when the energy demand is at minimum and at maximum when the energy demand is at maximum. In addition, analysis of the diesel price variability shows that the NPC and COE have different minimums. They increase as the diesel price increases and are at a different maximum when the diesel price is at maximum. Further variability analysis of discount rate shows that for the NPC, the discount rate is at minimum when the NPC is at maximum and at maximum when the NPC is at minimum. For the COE, the discount rate is at minimum when the COE is at minimum and at maximum when the COE is at maximum.

Putting the proposed model of the hybrid renewable energy configuration into practice in rural farm facilities will result in a reduced cost of energy production, adequate and increased accessibility to electricity, discourage rural-urban migration, increase food production, reduce the cost of food production, encourage investors to take to farming, improve the standard of living of rural residents and encourage urban-rural migration.

Future studies

Future research should conduct a comprehensive environmental impact assessment of hybrid renewable energy systems in agricultural settings, encompassing land use changes, biodiversity impacts, life-cycle analysis of components, effects on water resources and soil quality, noise and visual impacts, and strategies to mitigate negative effects while maximizing benefits. While this study utilized HOMER software for system optimization, future research could explore the application of alternative optimization techniques to further validate and potentially enhance the design of hybrid renewable energy systems for agricultural settings. Techniques such as Genetic Algorithms (GA), Particle Swarm Optimization (PSO), Mayfly Algorithm, CUKO Search, Gray Wolf Optimization, Harmony Search (HS), and Flower Pollination Algorithm (FPA) could be employed to optimize system configurations. A comparative analysis of these methods against HOMER results would provide valuable insights into the strengths and limitations of different optimization approaches in the context of rural farm energy systems. Such research could potentially uncover more nuanced optimal solutions, especially for complex system configurations or when considering additional constraints not easily modeled in HOMER. Furthermore, this comparative approach could lead to the development of new, hybrid optimization techniques specifically tailored for renewable energy systems in agricultural applications, potentially improving the accuracy and efficiency of system design processes.

Declaration of generative ai and ai assisted technologies in the writing process

During the preparation of this work, the authors used AI for synthesis of thought process, grammar check and spelling, clarity and conciseness, style and tone, and vocabulary enhancement. After using this tool/service, the authors reviewed and edited the content as needed and take full responsibility for the content of the publication.

CRediT authorship contribution statement

Michael Uzoamaka Emezirinwune: Writing – review & editing, Writing – original draft, Methodology, Data curation, Conceptualization. **Isaiah Adediji Adejumobi:** Writing – review & editing, Supervision. **Oluwaseun Ibrahim Adebisi:** Writing – review & editing, Supervision. **Festus Gboyega Akinboro:** Writing – review & editing, Supervision.

Declaration of competing interest

The authors affirm that they have no known financial or interpersonal conflicts that would have appeared to have an impact on the research presented in this paper.

Data availability

Data will be made available on request.

References

[1] M.U. Emezirinwune, I.A. Adejumobi, O.I. Adebisi, F.G. Akinboro, Synergizing hybrid renewable energy systems and sustainable agriculture for rural development in Nigeria, e-Prime - Adv. Electr. Eng., Electr. Energy 7 (2024) 100492, https://doi.org/10.1016/J.PRIME.2024.100492.
[2] F. Riva, H. Ahlborg, E. Hartvigsson, S. Pachauri, E. Colombo, Electricity access and rural development: review of complex socio-economic dynamics and causal diagrams for more appropriate energy modelling, Energy Sustain. Develop. 43 (2018) 203–223.
[3] EIA, "EIA projects nearly 50% increase in world energy usage by 2050, led by growth in Asia," 2019.
[4] D. Gielen et al., "Global energy transformation: a roadmap to 2050," 2019.
[5] N. Magnani, A. Vaona, Access to electricity and socio-economic characteristics: panel data evidence at the country level, Energy 103 (2016) 447–455.

[6] I. Noumba, S.M. Nguea, Assessing the role of globalization for universal electricity access, Int. Econ. 174 (2023) 180–195.
[7] W. Bank, "Access to Electricity, Rural (% of Rural Population) - Nigeria," World Bank Data.
[8] K.Q. Jimah, A.W. Isah, M.S. Okundamiya, Erratic and epileptic power supply in Nigeria: causes and Solutions, Adv. Electr. Telecommun. Eng. (AETE) 2 (1) (2019) 47–53. *ISSN: 2636-7416*.
[9] J. Adebisi, P. Ibili, M. Emezirinwune, K. Abdulsalam, Comparative study of hybrid solar photovoltaic-diesel power supply system, Afr. J. Inter/Multidisciplinary Stud. 5 (1) (2023) 1–15.
[10] O.M. Babatunde, C.O. Ayegbusi, D.E. Babatunde, P.O. Oluseyi, T.E. Somefun, Electricity supply in Nigeria: cost comparison between grid power tariff and fossil-powered generator, Int. J. Energy Econ. Policy 10 (2) (2019) 160–164.
[11] O.M. Babatunde, J.L. Munda, Y. Hamam, Hybridized off-grid fuel cell/wind/solar PV/battery for energy generation in a small household: a multi-criteria perspective, Int. J. Hydrogen. Energy 47 (10) (2022) 6437–6452.
[12] M.S. Okundamiya, Size optimization of a hybrid photovoltaic/fuel cell grid connected power system including hydrogen storage, Int. J. Hydrogen. Energy (2020).
[13] M.U. Emezirinwune, Design and construction of an automatic voltage regulator for a synchronous alternator, Sci. Bulletin Electr. Eng. Faculty 22 (1) (2022) 1–7.
[14] I.A. Adediran, K.O. Isah, A.E. Ogbonna, S.K. Badmus, A global analysis of the macroeconomic effects of climate change, Asian Econ. Lett. 4 (Early View) (2023).
[15] O.M. Babatunde, B.D. Akintayo, M.U. Emezirinwune, O.A. Olanrewaju, Environmental impact assessment of a 1 kW proton-exchange membrane fuel cell: a mid-point and end-point analysis, Hydrogen 5 (2) (2024) 352–373.
[16] S. Jain, R.K. Bargah, Environmental pollution and sustainable development, Enviro. Sustain. Develop. Perspect. Issues (2024) 52.
[17] D.E. Babatunde, O.M. Babatunde, M.U. Emezirinwune, I.H. Denwigwe, T. E. Okharedia, O.J. Omodara, Feasibility analysis of an off-grid photovoltaic-battery energy system for a farm facility, Int. J. Electr. Comput. Eng. (IJECE) 10 (3) (2020) 2874–2883.
[18] M.K.G. Deshmukh, M. Sameeroddin, D. Abdul, M.A. Sattar, Renewable energy in the 21st century: a review, Mater. Today: Proc. 80 (2023) 1756–1759.
[19] P. Fragkos, Assessing the energy system impacts of Morocco's nationally determined contribution and low-emission pathways, Energy Strategy Rev. 47 (2023) 101081.
[20] O. Babatunde, I. Denwigwe, O. Oyebode, D. Ighravwe, A. Ohiaeri, D. Babatunde, Assessing the use of hybrid renewable energy system with battery storage for power generation in a University in Nigeria, Enviro. Sci. Pollut. Res. 29 (3) (2022) 4291–4310.
[21] O.M. Babatunde, J.L. Munda, and Y. Hamam, "A comprehensive state-of-the-art survey on hybrid renewable energy system operations and planning," IEEE Access, 2020.
[22] Y.F. Nassar, et al., Assessing the viability of solar and wind energy technologies in semi-arid and arid regions: a case study of libya's climatic conditions, Appl. Solar Energy (English translation of Geliotekhnika) 60 (1) (2024) 149–170, https://doi.org/10.3103/S0003701X24600218.
[23] O.M. Babatunde, J.L. Munda, Y. Hamam, Power system flexibility: a review, Energy Rep. 6 (2020) 101–106.
[24] O.M. Babatunde, M.U. Emezirinwune, H. Denwigwel, J.T. Akin-Adeniyi, Hybrid power system for off-grid communities: techno-economic and energy mix analysis, in: Electro-Technology for National Development (NIGERCON), 2017 IEEE 3rd International Conference on, 2017, pp. 946–952.
[25] L. Charfeddine, M. Kahia, Do information and communication technology and renewable energy use matter for carbon dioxide emissions reduction? Evidence from the Middle East and North Africa region, J. Clean. Prod. 327 (2021) 129410.
[26] D. Jones, Global Electricity review2022, Ember, 2022.
[27] A.M. Barbosa, P.R. Junior, L.C.S. Rocha, A. de Souza Barbosa, I. Bolis, Optimization methods of distributed hybrid power systems with battery storage system: a systematic review, J. Energy Storage 97 (2024) 112909.
[28] A.K. Patwary, M.A. Sayem, M.A. Hossain, M.A. Halim, A Review of Energy Storage Systems (ESS) for Integrating Renewable Energies in Microgrids, Control Syst. Optimization Lett. 2 (1) (2024) 103–112.
[29] M. Faisal, M.A. Hannan, P.J. Ker, A. Hussain, M. Bin Mansor, F. Blaabjerg, Review of energy storage system technologies in microgrid applications: issues and challenges, IEEE Access. 6 (2018) 35143–35164.
[30] K. Ghanbari, A. Maleki, D.R. Ochbelagh, Optimal design of solar/wind/energy storage system-powered RO desalination unit: single and multi-objective optimization, Energy Convers. Manage 315 (2024) 118768.
[31] X. Fu, Z. Wei, H. Sun, Y. Zhang, Agri-energy-environment synergy-based distributed energy planning in rural areas, IEEe Trans. Smart. Grid. (2024).
[32] O.E.D. Zafar A. Khan, Muhammad Imran, Abdullah Altamimi, A.O. Abdelatif, Assessment of wind and solar hybrid energy for agricultural applications in Sudan, Energies. (Basel) 15 (5) (2021) 1–18.
[33] M.F. Elmorshedy, et al., Feasibility study and performance analysis of microgrid with 100% hybrid renewables for a real agricultural irrigation application, Sustain. Energy Technol. Assess. 53 (2022) 102746.
[34] H.O. Pandyaswargo, Andante Hadi, Alan Dwi Wibowo, "Socio-techno-economic assessment to design an appropriate renewable energy system for remote agricultural communities in developing countries, Sustain. Prod. Consum. 31 (2022) 492–511.
[35] K.C. Sanjay, M. Karthikeyan, K.M. Prasannakumaran, V. Kirubakaran, Techno commercial study of hybrid systems for the agriculture farm using homer software. Hybrid Renewable Energy Systems, 2021, pp. 115–133.
[36] S.S. Chandel, M.N. Naik, R. Chandel, Review of solar photovoltaic water pumping system technology for irrigation and community drinking water supplies, Renew. Sustain. Energy Rev. 49 (2015) 1084–1099.
[37] M.R. Elkadeem, S. Wang, S.W. Sharshir, E.G. Atia, Feasibility analysis and techno-economic design of grid-isolated hybrid renewable energy system for electrification of agriculture and irrigation area: a case study in Dongola, Sudan, Energy Convers. Manage 196 (2019) 1453–1478.
[38] M.R. Elkadeem, et al., Techno-economic design and assessment of grid-isolated hybrid renewable energy system for agriculture sector, in: 2019 14th IEEE Conference on Industrial Electronics and Applications (ICIEA), 2019, pp. 1562–1568.
[39] R.H.E. Hassanien, M. Li, W.D. Lin, Advanced applications of solar energy in agricultural greenhouses, Renew. Sustain. Energy Rev. 54 (2016) 989–1001.
[40] M. Bey, A. Hamidat, B. Benyoucef, T. Nacer, Viability study of the use of grid connected photovoltaic system in agriculture: case of Algerian dairy farms, Renew. Sustain Energy Rev. 63 (2016) 333–345.
[41] J. Carroquino, R. Dufo-López, J.L. Bernal-Agust\'\in, Sizing of off-grid renewable energy systems for drip irrigation in Mediterranean crops, Renew. Energy 76 (2015) 566–574.
[42] M. Frisk, "Simulation and Optimization of a Hybrid Renewable Energy System for application on a Cuban farm," 2017.
[43] F. Rinaldi, F. Moghaddampoor, B. Najafi, R. Marchesi, Economic feasibility analysis and optimization of hybrid renewable energy systems for rural electrification in Peru, Clean. Technol. Environ. Policy. (2020) 1–18.
[44] J. Li, P. Liu, Z. Li, Optimal design and techno-economic analysis of a solar-wind-biomass off-grid hybrid power system for remote rural electrification: a case study of west China, Energy (2020) 118387.
[45] K. Murugaperumal, S. Srinivasn, G.S. Prasad, Optimum design of hybrid renewable energy system through load forecasting and different operating strategies for rural electrification, Sustain. Energy Technol.Assess. 37 (2020) 100613.
[46] J. Ahmad, et al., Techno economic analysis of a wind-photovoltaic-biomass hybrid renewable energy system for rural electrification: a case study of Kallar Kahar, Energy 148 (2018) 208–234.
[47] A. Chatterjee, R. Rayudu, Techno-economic analysis of hybrid renewable energy system for rural electrification in India, in: 2017 IEEE Innovative Smart Grid Technologies-Asia (ISGT-Asia), 2017, pp. 1–5.
[48] S. Ladide, A. El Fathi, M. Bendaoud, H. Hihi, K. Faitah, Hybrid renewable power supply for typical public facilities in six various climate zones in Morocco, Int. J. Renew. Energy Res. (IJRER) 9 (2) (2019) 893–912.
[49] F. Fodhil, A. Hamidat, O. Nadjemi, Potential, optimization and sensitivity analysis of photovoltaic-diesel-battery hybrid energy system for rural electrification in Algeria, Energy 169 (2019) 613–624.
[50] M. Hossain, S. Mekhilef, L. Olatomiwa, Performance evaluation of a stand-alone PV-wind-diesel-battery hybrid system feasible for a large resort center in South China Sea, Malaysia, Sustain. Cities. Soc. 28 (2017) 358–366.
[51] L. Olatomiwa, S. Mekhilef, M.S. Ismail, M. Moghavvemi, Energy management strategies in hybrid renewable energy systems: a review, Renew. Sustain. Energy Rev. 62 (2016) 821–835.
[52] R. Siddaiah, R.P. Saini, A review on planning, configurations, modeling and optimization techniques of hybrid renewable energy systems for off grid applications, Renew. Sustain. Energy Rev. 58 (2016) 376–396.
[53] B. Bhandari, K.T. Lee, G.Y. Lee, Y.M. Cho, S.H. Ahn, Optimization of hybrid renewable energy power systems: a review, Int. J. Precision Eng. Manufact.-Green Technol. 2 (1) (2015) 99–112.
[54] F.A.O. IRENA, "Renewable energy for agri-food systems: towards the Sustainable Development Goals and the Paris Agreement," 2021.
[55] H. Hartung, L. Pluschke, The Benefits and Risks of Solar Powered Irrigation, Food and Agriculture Organization, RomeItaly, 2018.
[56] F.A.O. IRENA, "Renewable energy for agri-food systems: towards the Sustainable Development Goals and the Paris Agreement," 2021.
[57] G. of India, "Ministry of new and renewable energy (MNRE)," 2021.
[58] U. Nations, "Food and agriculture organization of the united nations," 2020.
[59] O.M. Babatunde, J.L. Munda, Y. Hamam, A comprehensive state-of-the-art survey on hybrid renewable energy system operations and planning, IEEe Access. 4 (2020) 75313–75346.
[60] H. Energy, 1790 30th St Suite 100, B. C. 80301 USA, +1-720-565-4046, 2016.
[61] J. Aldersey-Williams, T. Rubert, Levelised cost of energy–A theoretical justification and critical assessment, Energy policy 124 (2019) 169–179.
[62] H. Energy, 1790 30th St Suite 100, B. C. 80301 USA, +1-720-565-4046, 2016.
[63] L. Olatomiwa, R. Blanchard, S. Mekhilef, D. Akinyele, Hybrid renewable energy supply for rural healthcare facilities: an approach to quality healthcare delivery, Sustain. Energy Technol. Assess. 30 (2018) 121–138.
[64] T.P. Chang, F.J. Liu, H.H. Ko, S.P. Cheng, L.C. Sun, S.C. Kuo, Comparative analysis on power curve models of wind turbine generator in estimating capacity factor, Energy 73 (2014) 88–95.
[65] H. Yang, W. Zhou, L. Lu, Z. Fang, Optimal sizing method for stand-alone hybrid solar–wind system with LPSP technology by using genetic algorithm, Solar energy 82 (4) (2008) 354–367.
[66] R. Pallabazzer, Evaluation of wind-generator potentiality, Solar energy 55 (1) (1995) 49–59.
[67] Y. Wang, Z. Zhou, A. Botterud, K. Zhang, Optimal wind power uncertainty intervals for electricity market operation, IEEe Trans. Sustain. Energy 9 (1) (2017) 199–210.
[68] O.M. Babatunde, J.L. Munda, Y. Hamam, A comprehensive state-of-the-art survey on hybrid renewable energy system operations and planning, IEEe Access. (2020).

[69] O.M. Babatunde, J.L. Munda, Y. Hamam, Off-grid hybrid photovoltaic–micro wind turbine renewable energy system with hydrogen and battery storage: effects of sun tracking technologies, Energy Convers. Manage 255 (2022) 115335.

[70] Y.S. Mohammed, M.W. Mustafa, N. Bashir, Hybrid renewable energy systems for off-grid electric power: review of substantial issues, Renew. Sustain. Energy Rev. 35 (2014) 527–539.

[71] R. Dufo-Lopez, J.L. Bernal-Agustin, Multi-objective design of PV–wind–diesel–hydrogen–battery systems, Renew. Energy 33 (12) (2008) 2559–2572.

[72] S. Diaf, D. Diaf, M. Belhamel, M. Haddadi, A. Louche, A methodology for optimal sizing of autonomous hybrid PV/wind system, Energy policy 35 (11) (2007) 5708–5718.

[73] V. Suresh, M. Muralidhar, R. Kiranmayi, Modelling and optimization of an off-grid hybrid renewable energy system for electrification in a rural areas, Energy Rep. 6 (2020) 594–604.

[74] A. Gupta, R.P. Saini, M.P. Sharma, Modelling of hybrid energy system Part I: problem formulation and model development, Renew. Energy 36 (2) (2011) 459–465.

[75] O.M. Babatunde, J.L. Munda, Y. Hamam, Selection of a hybrid renewable energy systems for a low-income household, Sustainability. 11 (16) (2019) 4282.

[76] M. Abdunnabi, N. Etiab, Y.F. Nassar, H.J. El-Khozondar, R. Khargotra, Energy savings strategy for the residential sector in Libya and its impacts on the global environment and the nation economy, Adv. Build. Energy Res. 17 (4) (2023) 379–411, https://doi.org/10.1080/17512549.2023.2209094.

[77] O. Babatunde, D. Akinyele, T. Akinbulire, P. Oluseyi, Evaluation of a grid-independent solar photovoltaic system for primary health centres (PHCs) in developing countries, Renew. Energy Focus 24 (2018), https://doi.org/10.1016/j.ref.2017.10.005.

Michael Uzoamaka Emezirinwune received the B.Eng. degree in electrical/electronic engineering from the University of Port Harcourt, Port Harcourt, Nigeria, in 2009, and the M.Sc. degree in electrical/electronic engineering with a major in electrical power systems analysis from the University of Lagos, Akoka, Nigeria, in 2016 and currently studying for the PhD degree in electrical/electronic engineering with a major in electrical machines and power systems at the Federal University of Agriculture, Abeokuta, Nigeria. He has published scholarly articles in top-rated journals, and he is a registered professional engineer in Nigeria. **Email:** michaelemezirinwune@yahoo.com

Isaiah Adediji Adejumobi received the B.Eng., M.Eng. and Ph.D. degrees in Electrical Engineering from the University of Ilorin, Ilorin, Nigeria in 1987, 1992, and 2004 respectively. He started his academic career at the University of Ilorin in 1990 where he worked for about fifteen and half years before joining the services of the Federal University of Agriculture, Abeokuta (FUNAAB) in 2006. He became an Associate Professor in 2012 and a full Professor of Power System Engineering in 2015. He is a Corporate Member of the Nigerian Society of Engineers (NSE) and a Registered Engineer with the Council for the Regulation of Engineering in Nigeria (COREN). He is the 64th Inaugural Lecturer of FUNAAB and his inaugural lecture titled 'Electricity, Man and Development: The Complexity of the Distribution System Management in a Power Network' was delivered in June 2021. His research interests include power system network design and analysis, reliability assessment, harmonic analysis, and demand-side management among others. He has well over 80 journal articles and conference proceedings to his credit in the field of power system engineering. He can be contacted at email: adejumobiia@funaab.edu.ng

Oluwaseun Ibrahim Adebisi obtained his B.Eng., M.Eng. and Ph.D. degrees in Electrical and Electronics Engineering from the Federal University of Agriculture, Abeokuta (FUNAAB), Nigeria in 2010, 2013, and 2019 respectively. He specializes in power system engineering and electrical machines. He began his academic career in the Department of Electrical and Electronics Engineering, FUNAAB in 2011 as a Junior Research Fellow and he is currently a Senior Lecturer in the Department. He is a Corporate Member of the Nigerian Society of Engineers (NSE) and a Registered Engineer with the Council for the Regulation of Engineering in Nigeria (COREN). His research interests include web-based information exchange modeling for power system applications, power system network design and analysis, and electrical machines design among others. He can be contacted at email: adebisioluwaseun@funaab.edu.ng

Dr Akinboro Festus Gboyega, a Reader in the area of Environmental Physics with Ph.D. degree in Environmental Physics. He was involved in the design and construction of Electrical/Electronics, Instrumentation, Metal fabrication, Engineering machines and instruments since 1988; and had Award of Excellence from Ogun State government, Nigeria in the year 2004. Akinboro F. G. has constructed more than thirty (30) different types of Electrical, Electronics, Electromechanical Machines and controls at commercial level for various industrialists. His carrier in the area of Renewable Energy especially Solar started in 1995 as a Post Graduate Student (Solar Energy option) at the University of Lagos.